CMS

CMS-TOP-12-035

Measurement of the ratio $\mathcal{B}(\mathrm{t} \to \mathrm{Wb})/\mathcal{B}(\mathrm{t} \to \mathrm{Wq})$ in pp collisions at $\sqrt{s} = 8\,\mathrm{TeV}$

The CMS Collaboration[*]

Abstract

The ratio of the top-quark branching fractions $\mathcal{R} = \mathcal{B}(\mathrm{t} \to \mathrm{Wb})/\mathcal{B}(\mathrm{t} \to \mathrm{Wq})$, where the denominator includes the sum over all down-type quarks (q = b, s, d), is measured in the $\mathrm{t\bar{t}}$ dilepton final state with proton-proton collision data at $\sqrt{s} = 8\,\mathrm{TeV}$ from an integrated luminosity of $19.7\,\mathrm{fb}^{-1}$, collected with the CMS detector. In order to quantify the purity of the signal sample, the cross section is measured by fitting the observed jet multiplicity, thereby constraining the signal and background contributions. By counting the number of b jets per event, an unconstrained value of $\mathcal{R} = 1.014 \pm 0.003\,\text{(stat.)} \pm 0.032\,\text{(syst.)}$ is measured, in good agreement with the standard model prediction. A lower limit $\mathcal{R} > 0.955$ at the 95% confidence level is obtained after requiring $\mathcal{R} \leq 1$, and a lower limit on the Cabibbo–Kobayashi–Maskawa matrix element $|V_{\mathrm{tb}}| > 0.975$ is set at 95% confidence level. The result is combined with a previous CMS measurement of the *t*-channel single-top-quark cross section to determine the top-quark total decay width, $\Gamma_{\mathrm{t}} = 1.36 \pm 0.02\,\text{(stat.)}^{+0.14}_{-0.11}\,\text{(syst.)}\,\mathrm{GeV}$.

[*]See Appendix A for the list of collaboration members

1 Introduction

Because of its large mass [1], the top quark decays before fragmenting or forming an hadronic bound state [2]. According to the standard model (SM), the top quark decays through an electroweak interaction almost exclusively to an on-shell W boson and a b quark. The magnitude of the top-bottom charged current is proportional to $|V_{tb}|$, an element of the Cabibbo–Kobayashi–Maskawa (CKM) matrix. Under the assumption that the CKM matrix is unitary, $|V_{tb}|$ is expected to be close to unity and dominate over the off-diagonal elements, i.e. $|V_{tb}| \gg |V_{ts}|, |V_{td}|$. Thus, the decay modes of the top quark to lighter down-type quarks (d or s) are allowed, but highly suppressed. The indirect measurement of $|V_{tb}|$, from the unitarity constraint of the CKM matrix, is $|V_{tb}| = 0.999146^{+0.000021}_{-0.000046}$ [3]. Any deviation from this value or in the partial decay width of the top quark to b quarks, would indicate new physics contributions such as those from a new heavy up- and/or down-type quarks or a charged Higgs boson, amongst others [4]. Direct searches at the Large Hadron Collider (LHC) have set lower limits on the mass of these hypothetical new particles [5–15], and the observation of a SM Higgs boson candidate [16–18] places stringent constraints on the existence of a fourth sequential generation of quarks. These results support the validity of both the unitarity hypothesis and the 3×3 structure of the CKM matrix for the energy scale probed by the LHC experiments. However, other new physics contributions, including those described above, could invalidate the bounds established so far on $|V_{tb}|$ [3].

In this Letter, we present a measurement of $\mathcal{R} = \mathcal{B}(t \to Wb)/\mathcal{B}(t \to Wq)$, where the denominator includes the sum over the branching fractions of the top quark to a W boson and a down-type quark (q = b, s, d). Under the assumption of the unitarity of the 3×3 CKM matrix, it is possible to show [3] that $\mathcal{R} = |V_{tb}|^2$, and thus to indirectly measure $|V_{tb}|$. In addition, the combination of a determination of $\mathcal{R}$ and a measurement of the t-channel single-top cross section can provide an indirect measurement of the top-quark width (Γ_t) [19]. The most recent measurement of Γ_t based on this approach [20] is found to be compatible with the SM predictions with a relative uncertainty of approximately 22%. The value of $\mathcal{R}$ has been measured at the Tevatron, and the most precise result is obtained by the D0 Collaboration, where $\mathcal{R} = 0.90 \pm 0.04$ (stat.+syst.) [21] indicates a tension with the SM prediction. This tension is enhanced for the measurement in the $t\bar{t}$ dilepton decay channel, where both W bosons decay leptonically and $\mathcal{R} = 0.86^{+0.041}_{-0.042}$ (stat.) ± 0.035 (syst.) is obtained. The most recent measurement by the CDF Collaboration [22] is consistent with the SM prediction [3].

Owing to its purity, the $t\bar{t}$ dilepton channel is chosen for this measurement. Events are selected from the data sample acquired in proton-proton collisions at $\sqrt{s} = 8$ TeV by the Compact Muon Solenoid (CMS) experiment at the LHC during 2012. The integrated luminosity of the analyzed data sample is 19.7 ± 0.5 fb^{-1} [23]. The selected events are used to measure the $t\bar{t}$ production cross section by fitting the observed jet multiplicity distribution, constraining the signal and background contributions. The b-quark content of the events is inferred from the distribution of the number of b-tagged jets per event as a function of jet multiplicity for each of the dilepton channels. Data-based strategies are used to constrain the main backgrounds and the contributions of extra jets from gluon radiation in $t\bar{t}$ events. The $\mathcal{R}$ value is measured by fitting the observed b-tagged jet distribution with a parametric model that depends on the observed cross section, correcting for the fraction of jets that cannot be matched to a $t \to Wq$ decay. The model also depends on the efficiency for identifying b jets and discriminating them from other jets. Lastly, the measurement of $\mathcal{R}$ is combined with a previously published CMS result of the t-channel production cross section of single top quarks in pp collisions [24] to yield an indirect determination of the top-quark total decay width.

2   The CMS detector

The central feature of the Compact Muon Solenoid (CMS) apparatus is a superconducting solenoid of 6 m internal diameter, providing a magnetic field of 3.8 T. Within the superconducting solenoid volume are a silicon pixel and strip tracker, a lead tungstate crystal electromagnetic calorimeter (ECAL), and a brass/scintillator hadron calorimeter (HCAL), each composed of a barrel and two endcap sections. Muons are measured in gas-ionization detectors embedded in the steel flux-return yoke outside the solenoid. Extensive forward calorimetry complements the coverage provided by the barrel and endcap detectors.

The silicon tracker measures charged particles within the pseudorapidity range $|\eta| < 2.5$, where the pseudorapidity η is defined as $\eta = -\ln[\tan(\theta/2)]$ and θ is the polar angle of the trajectory of the particle with respect to the anticlockwise-beam direction. The tracker consists of 1440 silicon pixel and 15 148 silicon strip detector modules and is located in field of the superconducting solenoid. It provides an impact parameter resolution of $\approx 15\,\mu$m and a transverse momentum (p_T) resolution of about 1.5% for 100 GeV particles. The electron energy is measured by the ECAL and its direction is measured by the tracker. The mass resolution for $Z \to$ ee decays is 1.6% when both electrons are in the ECAL barrel, and 2.6% when both electrons are in the ECAL endcap [25]. Matching muons to tracks measured in the silicon tracker results in a p_T resolution between 1 and 10%, for p_T values up to 1 TeV. The jet energy resolution (JER) amounts typically to 15% at 10 GeV, 8% at 100 GeV, and 4% at 1 TeV [26].

A more detailed description can be found in Ref. [27].

3   Simulation of signal and background events

The top-quark pair production cross section has been calculated at next-to-next-to-leading order (NNLO) and next-to-next-to-leading log (NNLL) [28]. In proton-proton collisions at $\sqrt{s} = 8$ TeV, and for a top-quark mass of 173.3 GeV, the expected cross section is $\sigma_{NNLO+NNLL}(t\bar{t}) = 246\,^{+6}_{-8}$ (scale)$^{+6}_{-6}$ (PDF) pb, where the first uncertainty is from to the factorisation and renormalisation scales, and the second is from the parton distribution functions (PDFs). Signal events are simulated for a top-quark mass of 172.5 GeV with the leading-order (LO) Monte Carlo (MC) MADGRAPH (v5.1.3.30) [29] generator matched to PYTHIA (v6.426) [30], where the τ lepton decays are simulated with the TAUOLA package (v27.121.5) [31]. The CTEQ6L1 PDF set is used in the event generation [32]. Matrix elements describing up to three partons in addition to the $t\bar{t}$ pair are included in the generator used to produce the simulated signal samples. A correction to the simulated top-quark p_T is applied, based on the approximate NNLO computation [33]: the events are reweighted at the generator level to match the top-quark p_T prediction, and the full difference between the reweighted and unweighted simulations is assigned as a systematic uncertainty.

The most relevant background processes for the dilepton channel are from the production of two genuine isolated leptons with large p_T. This includes Drell–Yan (DY) production of charged leptons, i.e. from a Z/γ^* decay, which is modelled with MADGRAPH for dilepton invariant masses above 10 GeV, and it is normalised to a NNLO cross section of 4.393 nb, computed using FEWZ [34]. Single-top-quark processes are modelled at next-to-leading order (NLO) with POWHEG (v1.0, r1380) [35–39] using the CTEQ6M PDF set [32], and normalised to cross sections of 22.2 pb, 86.1 pb, and 5.6 pb for the tW, t-, and s- channel production, respectively, from Ref. [33]. Diboson processes are modelled with MADGRAPH, and normalised to the NLO cross section computed with MCFM [40]. The generation of WW, WZ, and ZZ pairs is normalised to inclusive cross sections of 54.8 pb, 33.2 pb, and 17.7 pb, respectively. For WZ and ZZ

pairs a minimum dilepton invariant mass of 12 GeV is required. The production of a W boson in association with jets, which includes misreconstructed and nonprompt leptons, is modelled with MADGRAPH and normalised to a total cross section of 36.3 nb computed with FEWZ. Multijet processes are also studied in simulation but are found to yield negligible contributions to the selected sample.

A detector simulation based on GEANT4 (v.9.4p03) [41, 42] is applied after the generator step for both signal and background samples. The presence of multiple interactions (pileup) per bunch crossing is incorporated by simulating additional interactions (both in-time and out-of-time with the collision) with a multiplicity matching that observed in the data. The average number of pileup events in the data is estimated to be 21 interactions per bunch crossing.

4 Event selection and background determination

The event selection is optimised for $t\bar{t}$ dilepton final states that contain two isolated oppositely charged leptons ℓ (electrons or muons), missing transverse energy (E_T^{miss}) defined below, and at least two jets. Events in which the electrons or muons are from intermediate τ lepton decays are considered as signal events. Dilepton triggers are used to acquire the data samples, where a minimum transverse momentum of 8 GeV is required for each of the leptons, and 17 GeV is required for at least one of the leptons. Electron-based triggers include additional isolation requirements, both in the tracker and calorimeter detectors.

All objects in each event are reconstructed with a particle-flow (PF) algorithm [43, 44]. Reconstructed electron and muon candidates are required to have $p_T > 20$ GeV and to be in the fiducial region $|\eta| \leq 2.4$ of the detector. A particle-based relative isolation parameter is computed for each lepton and corrected on an event-by-event basis for the contribution from pileup events. We require that the scalar sum of the p_T of all particle candidates reconstructed in an isolation cone built around the lepton's momentum vector is less than 15% (12%) of the electron (muon) transverse momentum. The isolation cone is defined using the radius $R = \sqrt{(\Delta\eta)^2 + (\Delta\phi)^2} = 0.4$, where $\Delta\eta$ and $\Delta\phi$ are the differences in pseudorapidity and azimuthal angle between the particle candidate and the lepton. For each event we require at least two lepton candidates originating from a single primary vertex. Among the vertices identified in the event, the vertex with the largest $\sum p_T^2$, where the sum runs over all tracks associated with the vertex, is chosen as the primary vertex. If more than two isolated leptons are found, the ambiguity is resolved by selecting the dilepton pair with the highest scalar sum of transverse momenta. Same-flavour dilepton pairs (ee or $\mu\mu$) compatible with $Z \to \ell\ell$ decays are removed by requiring $|M_Z - M_{\ell\ell}| > 15$ GeV, where M_Z is the Z boson mass [3] and $M_{\ell\ell}$ is the invariant mass of the dilepton system. For all dilepton channels it is further required that $M_{\ell\ell} > 12$ GeV in order to veto low-mass dilepton resonances.

Jets are reconstructed by clustering all the PF candidates using the anti-k_T algorithm [45] with a distance parameter of 0.5. Jet momentum is defined as the vector sum of all particle momenta in the jet, and in the simulation it is found to be within 5 to 10% of the hadron-level momentum over the entire p_T spectrum and detector acceptance. A correction is applied by subtracting the extra energy clustered in jets due to pileup, following the procedure described in Refs. [46, 47]. The energies of charged-particle candidates associated with other reconstructed primary vertices in the event are also subtracted. Jet energy scale (JES) corrections are derived from simulation, and are validated with *in-situ* measurements of the energy balance of dijet and photon+jet events [26]. Additional selection criteria are applied to each event to remove spurious jet-like features originating from isolated noise patterns in certain HCAL

regions. In the selection of $t\bar{t}$ events, at least two jets, each with a corrected transverse momentum $p_T > 30\,\text{GeV}$ and $|\eta| \leq 2.4$, are required. The jets must be separated from the selected leptons by $\Delta R(\ell, \text{jet}) = \sqrt{(\Delta\eta)^2 + (\Delta\phi)^2} \geq 0.3$ where $\Delta\eta$ and $\Delta\phi$ are the differences in pseudorapidity and azimuthal angle between the lepton and jet directions. Events with up to four jets, selected under these criteria, are used.

The magnitude of the vector sum of the transverse momenta of all particles reconstructed in the event is used as the estimator for the momentum imbalance in the transverse plane, E_T^{miss}. All JES corrections applied to the event are also propagated into the E_T^{miss} estimate. For the ee and $\mu\mu$ channels, $E_T^{\text{miss}} > 40\,\text{GeV}$ is required in order to reduce the contamination from lepton pairs produced through the DY mechanism in association with at least two jets.

The DY contribution to the same-flavour dilepton channels is estimated from the data after the full event selection through the modelling of the angle $\Theta_{\ell\ell}$ between the two leptons. The $\Theta_{\ell\ell}$ distribution discriminates between leptons produced in DY processes and leptons from the top-quark pair decay cascade. In the first case an angular correlation is expected, while in the second case the leptons are nearly uncorrelated. The probability distribution function for $\Theta_{\ell\ell}$ is derived from data using a DY-enriched control region selected after inverting the E_T^{miss} requirement of the standard selection. Studies of simulated events indicate that the shape of the $\Theta_{\ell\ell}$ distribution is well described with this method, and that the contamination from other processes in the control region can be neglected. Compatibility tests performed in simulations using different channels and jet multiplicities are used to estimate an intrinsic 10% uncertainty in the final DY background. The other sources of uncertainty in the method are related to the simulation-based description of the probability distribution function for the $\Theta_{\ell\ell}$ distribution from other processes. Uncertainties are estimated either by propagating the uncertainties in pileup or JES and JER, or by trying alternative functions for the $t\bar{t}$ contribution with varied factorisation/renormalisation scales (μ_R/μ_F) with respect to their nominal values given by the momentum transfer in the event, matrix element/parton shower (ME-PS) matching threshold, or generator choice (POWHEG vs. MADGRAPH). The shapes of kinematic distributions for DY and other processes are used in a maximum-likelihood fit to estimate the amount of DY background in the selected sample. A total uncertainty of 21% is estimated from the data in the rate of DY events for the same-flavour channels.

For the eμ channel, a similar fit procedure is adopted using a different variable: the transverse mass $M_T = \sqrt{2E_T^{\text{miss}}p_T(1 - \cos\Delta\phi)}$ of each lepton, where $\Delta\phi$ is the difference in azimuthal angle between the lepton and the missing transverse momentum. The distribution of the sum $\sum M_T$ is used as the distribution in the fit. In this case the probability distribution function for $Z/\gamma^* \to \tau\tau \to \text{e}\mu$ is derived from simulation. The determination of the uncertainty associated with this method follows a similar prescription to that described above for the same-flavour channels. A total uncertainty of 21% is assigned to the amount of DY contamination in the eμ channel.

The second-largest background contribution is from single-top-quark processes (in particular the tW channel) that is relevant for this measurement since the decay products of a single top quark (instead of a pair) are selected. The contribution of this process is estimated from simulation. Uncertainties in the normalisation stemming from instrumental uncertainties in the integrated luminosity, trigger and selection efficiencies, and energy scales, as well as generator-specific uncertainties, are taken into account.

Table 1 shows the yields in the data and those predicted for signal and background events after the full event selection. The systematic uncertainties assigned to the predictions of signal and background events include the uncertainties in the JES and JER, pileup modelling, cross

Table 1: Predicted and observed event yields after the full event selection. The combination of statistical uncertainties with experimental and theoretical systematic uncertainties is reported. Non dileptonic $t\bar{t}$ channels, as well as associated production with vector bosons (W or Z), is designated as "Other $t\bar{t}$" and grouped with the expected contribution from single W boson and multijets productions. The expected contribution from vector boson pair processes is designated as "VV".

Source	ee	$\mu\mu$	eμ
W $\to \ell\nu$, multijets, other $t\bar{t}$	134 ± 91	43 ± 10	$(38 \pm 20) \times 10$
VV	292 ± 15	333 ± 16	995 ± 39
Z/$\gamma^* \to \ell\ell$	$(297 \pm 63) \times 10$	$(374 \pm 79) \times 10$	$(184 \pm 39) \times 10$
Single top quark	526 ± 26	583 ± 26	1834 ± 64
$t\bar{t}$ dileptons (signal)	$(1003 \pm 50) \times 10$	$(1104 \pm 54) \times 10$	$(349 \pm 17) \times 10^2$
Total	$(1395 \pm 81) \times 10$	$(1574 \pm 96) \times 10$	$(400 \pm 17) \times 10^2$
Data	13723	15596	38892

section calculations, integrated luminosity, and trigger and selection efficiencies. A conservative uncertainty is assigned to the predicted yields of multijet and W $\to \ell\nu$ background events since these contributions are from misidentified leptons and have been estimated solely from simulation. Good overall agreement is observed for all three dilepton categories between the yields in data and the sum of expected yields.

5 Cross section measurement

The selected events are categorized by the dilepton channel and the number of observed jets. Figure 1 shows the expected composition for each event category. Good agreement is observed between the distributions from the data and the expectations, including the control regions, defined as events with fewer than two or more than four jets. The chosen categorization not only allows one to study the contamination from initial- and final-state gluon radiation (ISR/FSR) in the sample, but also to constrain some of the uncertainties from the data.

The $t\bar{t}$ dilepton signal strength, μ, defined as the ratio of the observed to the expected signal rate, is measured from the jet multiplicity distribution by using a profile likelihood method [48]. A likelihood is calculated from the observed number of events in the k-different dilepton channels and jet multiplicity categories as

$$\mathcal{L}(\mu,\theta) = \prod_k \mathcal{P}\left[N_k, \hat{N}_k(\mu,\theta_i)\right] \cdot \prod_i \rho(\theta_i), \qquad (1)$$

where $\mathcal{P}$ is the Poisson probability density function, N_k is the number of events observed in the kth category, $\hat{N}_k$ is the total number of expected events from signal and background, and θ_i are the nuisance parameters, distributed according to a probability density function ρ. The nuisance parameters are used to modify the expected number of events according to the different systematic uncertainty sources, which include instrumental effects (such as integrated luminosity, pileup, energy scale, trigger and selection efficiencies) and signal modelling (μ_R/μ_F, PDF, ME-PS scale, top-quark mass, leptonic branching fractions of the W boson) amongst others. The uncertainty from the choice of the $t\bar{t}$ signal generator is estimated by assigning the difference between the MADGRAPH-based and the POWHEG-based predictions as an extra uncertainty in the fit. The nuisance parameters are assumed to be unbiased and distributed according to a log-normal function. Based on the likelihood expressed in Eq. (1), the profile likelihood ratio
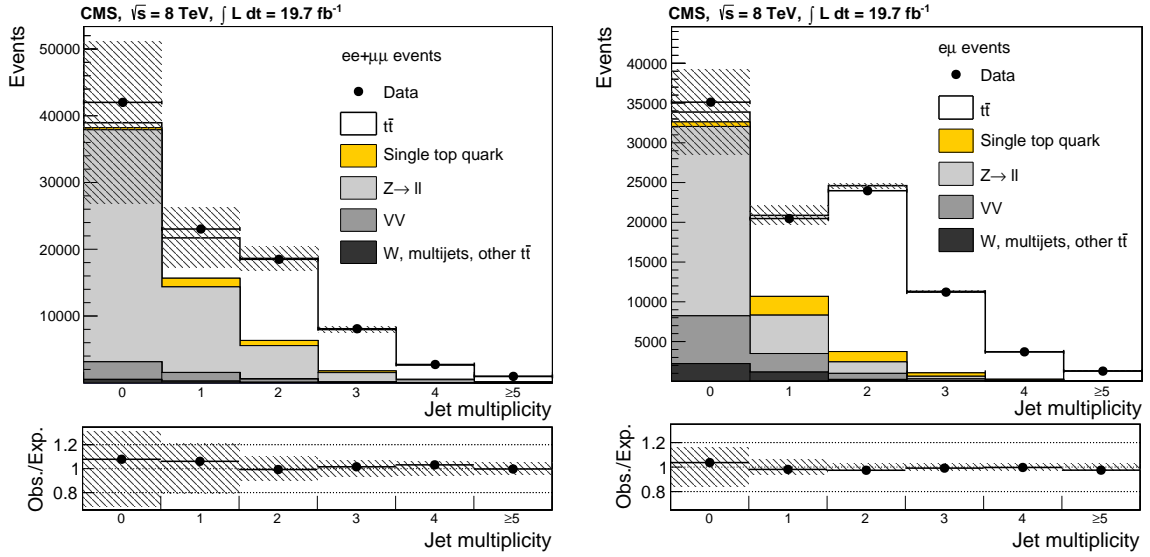
Figure 1: The upper plots show the observed jet multiplicity after the full event selection, except for the requirement on the number of jets, in the same-flavour (*left*) and different-flavour (*right*) channels. The simulated expectations are shown as stacked histograms, while the observed data distributions are represented as closed circles. The predicted distributions for the simulated $t\bar{t}$ and single-top-quark events correspond to a scenario with $\mathcal{R} = 1$. The lower panels show the ratio of the data to the expectations. The shaded bands represent the systematic uncertainty in the determination of the main background (DY) and the integrated luminosity.

(PLR) λ is defined as

$$\lambda(\mu) = \frac{\mathcal{L}(\mu, \hat{\hat{\theta}})}{\mathcal{L}(\hat{\mu}, \hat{\theta})}, \tag{2}$$

where the denominator has estimators $\hat{\mu}$ and $\hat{\theta}$ that maximise the likelihood, and the numerator has estimators $\hat{\hat{\theta}}$ that maximise the likelihood for the specified signal strength μ. The signal strength is obtained after maximising $\lambda(\mu)$ in Eq. (2). This approach allows us to parameterise the effect of the systematic uncertainties in the fit.

The signal strength μ is determined independently in each category, i.e. for each dilepton channel and jet multiplicity. For each category, the purity of the selected sample ($f_{t\bar{t}}$) is defined as the fraction of "true" $t\bar{t}$ signal events in the selected sample, $f_{t\bar{t}} = \mu \cdot N_{t\bar{t} \, \text{exp}} / N_{\text{obs}}$, where $N_{t\bar{t} \, \text{exp}}$ is the number of expected $t\bar{t}$ events, and N_{obs} is the total number of observed events. By performing the fit for each category, the purity of the sample is obtained. The results are summarized in Table 2. As expected, the $e\mu$ category has the highest purity ($\approx$90%). Because of the contamination from DY events, the same-flavour channels have lower purity ($\approx$70%). Overall, the signal purity increases with higher jet multiplicity.

As a cross-check, a fit including all categories, gives the range $0.909 < \mu < 1.043$ at the 68% confidence level (CL). This leads to a $t\bar{t}$ production cross section of

$$\sigma(t\bar{t}) = 238 \pm 1 \, (\text{stat.}) \pm 15 \, (\text{syst.}) \, \text{pb},$$

in good agreement with NNLO+NNLL expectation [28] and the latest CMS measurement [49]. An extra uncertainty is assigned in the extrapolation of the cross section to the full phase space because of the dependence of the acceptance on μ_R / μ_F, ME-PS threshold choices, and the top-quark mass.

Table 2: Fraction of $t\bar{t}$ events ($f_{t\bar{t}}$) and relative contribution from single-top-quark processes (k_{st}) for various jet multiplicities and dilepton channels, as determined from the profile likelihood fit. The total uncertainty is shown.

Parameter	Jet multiplicity	Dilepton channel		
		ee	$\mu\mu$	eμ
	2	0.67 ± 0.07	0.65 ± 0.08	0.85 ± 0.06
$f_{t\bar{t}}$	3	0.79 ± 0.06	0.78 ± 0.07	0.9 ± 0.07
	4	0.81 ± 0.11	0.82 ± 0.11	0.94 ± 0.10
	2	0.062 ± 0.004	0.063 ± 0.004	0.062 ± 0.003
k_{st}	3	0.040 ± 0.003	0.040 ± 0.003	0.041 ± 0.002
	4	0.036 ± 0.004	0.036 ± 0.006	0.029 ± 0.003

The relative single-top-quark contribution (k_{st}), defined as the ratio of the expected number of single-top-quark events to the estimated number of inclusive $t\bar{t}$ events, is also shown in Table 2 for each category. For this determination we use the expected number of single-top-quark events obtained after maximising the PLR in Eq. (2). The contribution due to single-top-quark events tends to be most significant in the two-jet category ($< 7\%$ relative to inclusive $t\bar{t}$ events). Since the estimate is obtained for a specific scenario in which $\mathcal{R} = 1$, an extra linear dependency of k_{st} on $\mathcal{R}$ is introduced in order to account for the increase in the tW cross section as $|V_{tb}|$ becomes smaller than $|V_{td}|$ or $|V_{ts}|$ [4]. In this parameterisation, the measured ratio $|V_{td}|/|V_{ts}| = 0.211 \pm 0.006$ is used [3], and the uncertainty is considered as an intrinsic systematic uncertainty in the measurement of $\mathcal{R}$.

6   Probing the heavy-flavour content

In this section the b-flavour content of the selected events (both signal and background) is determined from the b-tagged jet multiplicity distribution. The probability of incorrectly assigning a jet must be evaluated (Section 6.1) in order to correctly estimate the heavy-flavour content of top-quark decays (Section 6.2).

The b-tagging algorithm that is used (the combined secondary vertex, CSV method described in Ref. [50]) is a multivariate procedure in which both information on the transverse impact parameter with respect to the primary vertex of the associated tracks, and the reconstructed secondary vertices is used to discriminate b jets from c, light-flavour (u, d, s) and gluon jets. The b-tagging efficiency (ε_b) is measured [51] using multijet events where a muon is reconstructed inside a jet; a data-to-simulation scale factor is derived and is used to correct the predicted ε_b value in the $t\bar{t}$ dilepton sample from simulation. After correction, the expected efficiency in the selected $t\bar{t}$ sample is $\approx 84\%$, and the uncertainty in the scale factor from the data is 1–3%, depending on the kinematics of the jets [51]. The same scale factor is applied to the expected c-tagging efficiency but with a doubled uncertainty with respect to the one assigned to b jets owing to the fact that no direct measurement of the c-tagging efficiency is performed. For jets originating from the hadronisation of light-flavour jets, the misidentification efficiency (ε_q) is evaluated [50] from so-called negative tags in jet samples, which are selected using tracks that have a negative impact parameter or secondary vertices with a negative decay length. The scalar product of the vector pointing from the primary vertex to the point of closest approach of a track with negative impact parameter has the opposite sign of the scalar product taken with respect to the point of closest approach with the jet direction. The data-to-simulation correction factor for the misidentification efficiency is known with an uncertainty of about 11%, and the expected misidentification efficiency in the selected sample is approximately 12% [51].

Figure 2 shows the number of b-tagged jets in the selected dilepton data sample, compared to the expectations from simulation. The multiplicity is shown separately for each dilepton channel and jet multiplicity. The expected event yields are corrected after the PLR fit for the signal strength (described in the previous section) and also incorporate the data-to-simulation scale factors for ε_b and ε_q. Data and simulation agree within 5%. The residual differences can be related to the different number of jets selected from top-quark decays in data and simulation, and the modelling of gluon-radiative processes (ISR/FSR).
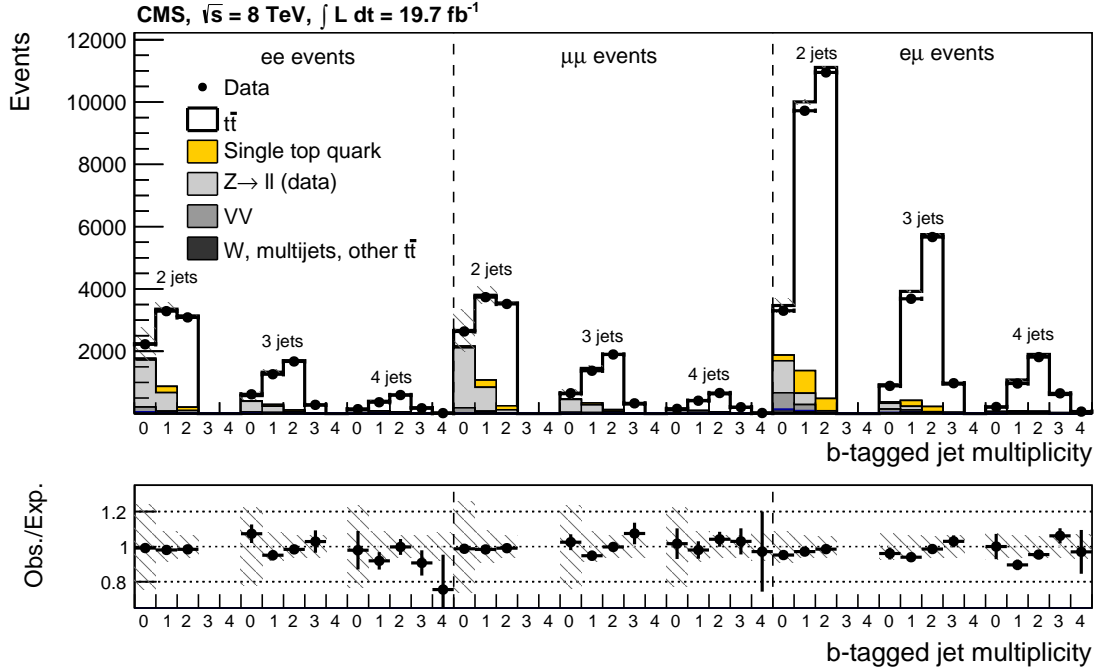
Figure 2: The upper plot shows the number of b-tagged jets per event for the different $t\bar{t}$ dilepton channels. For each final state, separate subsets are shown corresponding to events with two, three, or four jets. The simulated $t\bar{t}$ and single-top-quark events correspond to a scenario with $\mathcal{R} = 1$. The lower panel shows the ratio of the data to the expectations. The shaded bands represent the uncertainty owing to the finite size of the simulation samples, the main background contribution (DY), and the integrated luminosity.

6.1   Jet misassignment

There is a non-negligible probability that at least one jet from a $t\bar{t}$ decay is missed, either because it falls outside of the detector acceptance or is not reconstructed, and another jet from a radiative process is chosen instead. In the following discussion, this is referred to as a "misassigned jet". Conversely, jets that come from a top-quark decay will be referred to as "correctly assigned". The rate of correct jet assignments is estimated from the data using a combination of three different categories:

- events with no jets selected from top-quark decays, which also includes background events with no top quarks;
- events with only one jet from a top-quark decay, which includes some $t\bar{t}$ events and single-top-quark events (mainly produced through the tW channel);
- events with two jets produced from the two top-quark decays.

In order to avoid model uncertainties, the number of selected jets from top-quark decays is derived from the lepton-jet invariant-mass ($M_{\ell j}$) distribution, reconstructed by pairing each

lepton with all selected jets. For lepton-jet pairs originating from the same top-quark decay, the endpoint of the spectrum occurs at $M_{\ell j} \approx \sqrt{M_T^2 - m_W^2} \approx 153\,\text{GeV}$ [52], where M_T (m_W) is the top-quark (W boson) mass (Fig. 3, *left*, open histogram). The predicted distribution for correct pairings is obtained after matching the simulated reconstructed jets to the b quarks from $t \rightarrow Wb$ at the generator level using a cone of radius $R = 0.3$. The same quantity calculated for a lepton from a top-quark decay paired with a jet from the top antiquark decay and vice versa ("wrong" pairing) shows a distribution with a long tail (Fig. 3, *left*, filled histogram), which can be used as a discriminating feature. A similar tail is observed for "unmatched" pairings: either background processes without top quarks, or leptons matched to other jets. The combinations with $M_{\ell j} > 180\,\text{GeV}$ are dominated by incorrectly paired jets, and this control region is used to normalise the contribution from background.
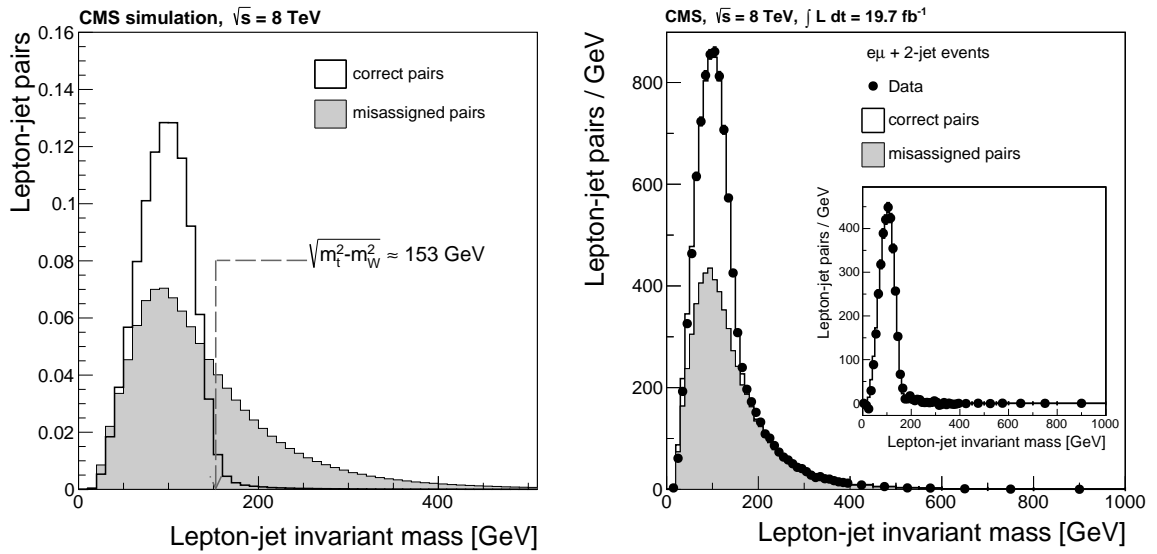
Figure 3: The left plot shows the correct and misassigned lepton-jet invariant-mass spectra in simulated $t\bar{t}$ dilepton events. Both distributions are normalised to unity. The endpoint of the spectrum for correctly assigned pairs is shown by the dashed line. In the right plot the observed data is compared with the correct (from simulation) and misassigned (from the data) components for the lepton-jet invariant-mass spectra in $e\mu$ events with exactly two jets. The lepton-jet mass distribution is shown in the inset, after the misassigned pairs are subtracted.

In order to model the lepton-jet invariant-mass distribution of the misassigned jets, an empirical method is used based on the assumption of uncorrelated kinematics. The validity of the method has been tested using simulation. For each event in data, the momentum vector of the selected lepton is "randomly rotated" with uniform probability in the $(\cos(\theta), \phi)$ phase space, and the $M_{\ell j}$ is recomputed. This generates a combinatorial distribution that is used to describe the true distribution of $M_{\ell j}$ for misassigned jets. Figure 3 (*right*) compares the data distribution with the two components of the $M_{\ell j}$ spectrum, i.e. "correct assignments" from simulation and "wrong assignments" modelled from the data. The background model provides a good estimate of the shape of the spectrum of the misassigned lepton-jet pairs. After fitting the fractions of the two components to the data, the "misassigned" contribution is subtracted from the inclusive spectrum, and the result is compared to the expected contribution from the correctly assigned lepton-jet pairs. The result of this procedure is shown in the inset of Fig. 3 (*right*). This method is used to determine the fraction (f_{correct}) of selected jets from top-quark decays in the $M_{\ell j}$ spectrum. Consequently, by measuring f_{correct}, we estimate directly from the data the number of top-quark decays reconstructed and selected. Notice that f_{correct} cannot be larger

Table 3: Fraction of lepton-jet pairs correctly assigned in the selected events estimated from the data and predicted from simulation. The last column shows the ratio of the fraction measured in data to the prediction from simulation. The total uncertainty is shown.

Dilepton channel	# jets	$f_{\text{correct}}^{\text{data}}$	$f_{\text{correct}}^{\text{MC}}$	data/MC
	2	0.28 ± 0.05	0.277 ± 0.001	1.03 ± 0.19
ee	3	0.22 ± 0.07	0.223 ± 0.001	0.99 ± 0.29
	4	0.19 ± 0.07	0.175 ± 0.001	1.09 ± 0.43
	2	0.28 ± 0.06	0.276 ± 0.001	1.00 ± 0.21
$\mu\mu$	3	0.24 ± 0.06	0.227 ± 0.001	1.05 ± 0.25
	4	0.20 ± 0.07	0.181 ± 0.001	1.08 ± 0.37
	2	0.36 ± 0.06	0.3577 ± 0.0007	1.01 ± 0.16
$e\mu$	3	0.26 ± 0.05	0.2625 ± 0.0007	1.00 ± 0.18
	4	0.21 ± 0.06	0.2047 ± 0.0008	1.00 ± 0.27

than $1/n$ for events with n jets, as it includes the combinatorial contribution by definition.

In Table 3 the values of f_{correct} found in the data are compared to those predicted from simulation. These include both the contamination from background events as well as the effect of missing one or two jets from top-quark decays after selection. The systematic uncertainties affecting the estimate of f_{correct} can be split into two sources:

- distortion of the $M_{\ell j}$ shape due to the JES and JER of the reconstructed objects [26];
- calibration uncertainties (derived in the previous section) owing to the uncertainty in the μ_R/μ_F scale, the simulation of gluon radiation and the underlying event, the top-quark mass value used in simulation, and the contributions from background processes.

For each case the fit is repeated with different signal probability distribution functions. The systematic uncertainty is estimated to be 3–10%, depending on the jet multiplicity in the event, and is dominated by the ME-PS matching threshold and the μ_R/μ_F scale uncertainties.

By combining the measured f_{correct} from the data with the fraction of $t\bar{t}$ and single-top-quark events, a parameterisation of the three classes of events is obtained: i.e. the number of events with 0, 1, or 2 selected top-quark decays. The relative amounts of the three event classes are parameterised by the probabilities α_i, where i corresponds to the number of jets from top-quark decays selected in an event. The probabilities α_i are constrained to $\sum_i \alpha_i = 1$. Figure 4 summarizes the values of α_i obtained for the individual event categories, where the differences are dominated by the event selection efficiencies and the background contribution in each category.

6.2 Heavy-flavour content

For a given number of correctly reconstructed and selected jets, the expected b-tagged jet multiplicity can be modelled as a function of $\mathcal{R}$ and the b-tagging and misidentification efficiencies. In the parameterisation, we distinguish events containing jets from 0, 1, or 2 top-quark decays. The model is an extension of the one proposed in Ref. [53]. For illustration, the most significant case is considered, i.e. modelling the observation of two b-tagged jets in an event with two reconstructed jets. For the case where two jets from top-quark decays are selected in the event, the probability to observe two b-tagged jets can be written as

$$P_{2j,2t,2d} = \mathcal{R}^2\varepsilon_b^2 + 2\mathcal{R}(1-\mathcal{R})\varepsilon_b\varepsilon_q + (1-\mathcal{R})^2\varepsilon_q^2, \tag{3}$$

where the subscripts (2j, 2t, 2d) indicate a two-jet event, with two b-tagged jets, and two top-quark decays. If instead, only one jet from a top-quark decay is present in the event, the proba-
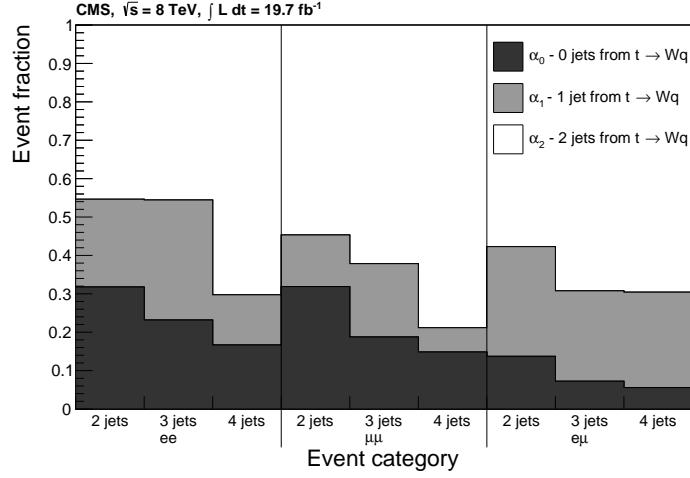
Figure 4: Fraction of events with 0, 1, or 2 top-quark decays selected, as determined from the data: these fractions, shown for different event categories, are labeled α_0, α_1, and α_2, respectively.

bility is modified to take the second jet into account in the measurement of $\mathcal{R}$. In this case, the probability of observing two b-tagged jets is

$$P_{2j,2t,1d} = \mathcal{R}^2 \varepsilon_b \varepsilon_{q*} + \mathcal{R}(1 - \mathcal{R})(\varepsilon_b + \varepsilon_q)\varepsilon_{q*} + (1 - \mathcal{R})^2 \varepsilon_q \varepsilon_{q*}, \qquad (4)$$

where ε_{q*} is the effective misidentification rate, and is computed by taking into account the expected flavour composition of the "extra" jets in the events (i.e. those not matched to a top-quark decay). The effective misidentification rate is derived specifically for each event category. From simulation, these extra jets are expected to come mostly from light-flavour jets ($\approx 87\%$). For completeness, for the case in which no jet from top-quark decay is reconstructed, the probability of observing two b-tagged jets is

$$P_{2j,2t,0d} = \varepsilon_{q*}^2. \qquad (5)$$

For each dilepton channel and jet multiplicity, analogous expressions are derived and combined using the probabilities α_i of having i reconstructed jets from top-quark decays. Additional terms are added to extend the model to events with more than two jets. All efficiencies are determined per event category, after convolving the corrections from dijet events in the data with the expected efficiencies (ε_q and ε_b) and the simulated jet p_T spectrum.

For the measurement of $\mathcal{R}$, a binned-likelihood function is constructed using the model described above and the observed b-tagging multiplicity in events with two, three, or four observed jets in the different dilepton channels. A total of 36 event categories, corresponding to different permutations of three lepton-flavour pairs, three jet multiplicities, and up to four observed b-tagged jets are used (see Fig. 2). The likelihood is generically written as

$$\mathcal{L}(\mathcal{R}, f_{t\bar{t}}, k_{st}, f_{correct}, \varepsilon_b, \varepsilon_q, \varepsilon_{q*}, \theta_i) = \prod_{\ell\ell} \prod_{N_{jets} \geq 2} \prod_{k=0}^{N_{jets}} \mathcal{P}[N_{ev}^{\ell\ell,N_{jets}}(k), \hat{N}_{ev}^{\ell\ell,N_{jets}}(k)] \prod_i \mathcal{G}(\theta_i^0, \theta_i, 1), \quad (6)$$

where $N_{ev}^{\ell\ell,N_{jets}}$ ($\hat{N}_{ev}^{\ell\ell,N_{jets}}$) is the number of observed (expected) events with k b-tagged jets in a given dilepton channel ($\ell\ell = ee, \mu\mu, e\mu$) with a given jet multiplicity (N_{jets}), θ_i are the nuisance parameters (a total of 33, which will be discussed later), and $\mathcal{G}$ is a Gaussian distribution. For

the nominal fit, the nuisance parameters are assumed to be unbiased ($\theta_i^0 = 0$) and normally distributed. The nuisance parameters parameterise the effect of uncertainties, such as JES and JER, b-tagging and misidentification rates, and μ_R/μ_F scales, amongst others, on the input parameters of the likelihood function. The most likely value for $\mathcal{R}$ is found after profiling the likelihood using the same technique described in Section 5.

6.3   Measurement of $\mathcal{R}$

In the fit, $\mathcal{R}$ is allowed to vary without constraints. The parameters of the model are all taken from the data: $f_{t\bar{t}}$ and k_{st} are taken from Table 2, $f_{correct}$ is taken from Table 3, ε_b and ε_q from dijet-based measurements [50], and ε_{q*} is derived following the method described in the previous section. Figure 5 shows the resulting prediction for the fraction of events with different numbers of observed b-tagged jets as a function of $\mathcal{R}$. The individual predictions for all categories are summed to build the inclusive model for the observation of up to four b-tagged jets in the selected events.
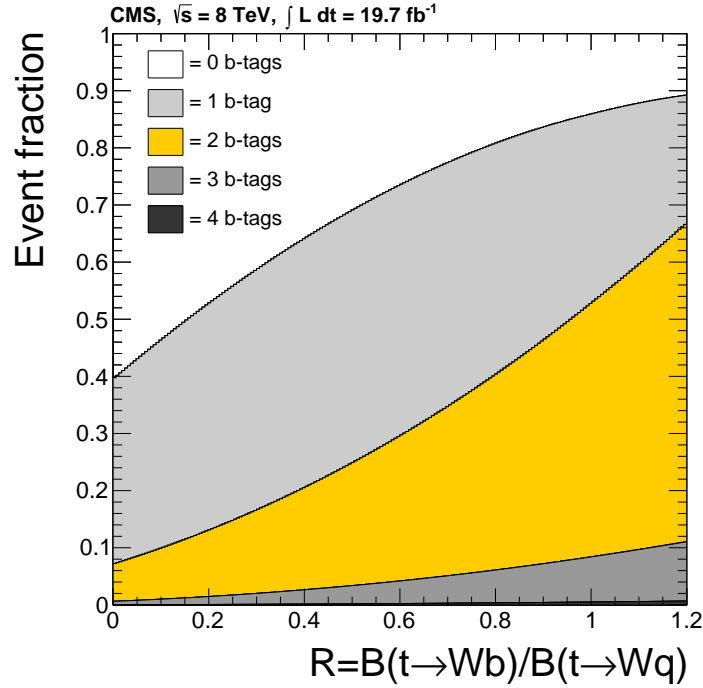
Figure 5: Expected event fractions of different b-tagged jet multiplicities in dilepton events as a function of $\mathcal{R}$.

Figure 6 shows the results obtained by maximising the profile likelihood. The combined measurement of $\mathcal{R}$ gives $\mathcal{R} = 1.014 \pm 0.003\,\text{(stat.)} \pm 0.032\,\text{(syst.)}$, in good agreement with the SM prediction. Fits to the individual channels give consistent results. For these, we obtain values of $\mathcal{R}_{ee} = 0.997 \pm 0.007\,\text{(stat.)} \pm 0.035\,\text{(syst.)}$, $\mathcal{R}_{\mu\mu} = 0.996 \pm 0.007\,\text{(stat.)} \pm 0.034\,\text{(syst.)}$, and $\mathcal{R}_{e\mu} = 1.015 \pm 0.003\,\text{(stat.)} \pm 0.031\,\text{(syst.)}$ for the ee, $\mu\mu$, and eμ channels, respectively. The measurement in the eμ channel dominates in the final combination since the main systematic uncertainties are fully correlated and this channel has the lowest statistical uncertainty.

The total relative uncertainty in the measurement of $\mathcal{R}$ is 3.2%, and is dominated by the systematic uncertainty, whose individual contributions are summarized in Table 4. The largest contribution to the systematic uncertainty is from the b-tagging efficiency measurement. Additional sources of uncertainty are related to the determination of the purity of the sample ($f_{t\bar{t}}$)
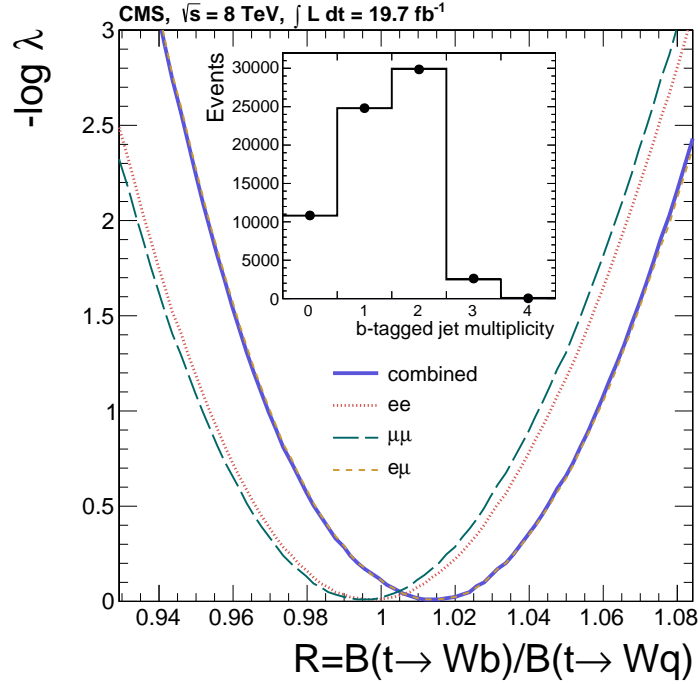
Figure 6: Variation of the log of the profile likelihood ratio (λ) used to extract $\mathcal{R}$ from the data. The variations observed in the combined fit and in the exclusive ee, $\mu\mu$, and eμ channels, are shown. The inset shows the inclusive b-tagged jet multiplicity distribution and the result of the fit.

and the fraction of correct assignments ($f_{correct}$) from the data; these quantities are affected by theoretical uncertainties related to the description of t$\bar{\text{t}}$ events, which have similar impact on the final measurement, such as μ_R/μ_F, ME-PS, signal generator, top-quark mass, and top-quark p_T. Instrumental contributions from JES and JER, modelling of the unclustered E_T^{miss} component in simulation, and the contribution from the DY and misidentified-lepton backgrounds are each estimated to contribute a relative systematic uncertainty $<0.6\%$. Another source of uncertainty is due to the contribution from extra sources of heavy-flavour production, either from gluon splitting in radiated jets or from decays in background events such as W $\rightarrow$ c$\bar{\text{s}}$. This effect has been estimated in the computation of ε_{q*} by assigning a conservative uncertainty of 100% to the c and b contributions. The effect of the uncertainty in the misidentification efficiency is estimated to be small ($<1\%$), as well as other sources of uncertainty, such as pileup and integrated luminosity.

If the three-generation CKM matrix is assumed to be unitary, then $\mathcal{R} = |V_{tb}|^2$ [4]. By performing the fit in terms of $|V_{tb}|$, a value of $|V_{tb}| = 1.007 \pm 0.016$ (stat.+syst.) is measured. Upper and lower endpoints of the 95% CL interval for $\mathcal{R}$ are extracted by using the Feldman–Cousins (FC) frequentist approach [54]. The implementation of the FC method in ROOSTATS [55] is used to compute the interval. All the nuisance parameters (including ε_b) are profiled in order to take into account the corresponding uncertainties (statistical and systematic). If the condition $\mathcal{R} \leq 1$ is imposed, we obtain $\mathcal{R} > 0.955$ at the 95% CL. Figure 7 summarizes the expected limit bands for 68% CL, 95% CL, and 99.7% CL, obtained from the FC method. The expected limit bands are determined from the distribution of the profile likelihood obtained from simulated pseudo-experiments. The upper and lower acceptance regions constructed in this procedure are used to determine the endpoints on the allowed interval for $\mathcal{R}$. In the pseudo-experiments the expected signal and background yields are varied using Poisson probability distributions

Table 4: Summary of the systematic uncertainties affecting the measurement of $\mathcal{R}$. The values of the uncertainties are relative to the value of $\mathcal{R}$ obtained from the fit.

Source	Uncertainty (%)
Experimental uncertainties:	
ε_b	2.4
ε_q	0.4
$f_{t\bar{t}}$	0.1
DY	0.2
misidentified lepton	0.1
JER	0.5
JES	0.5
unclustered E_T^{miss}	0.5
integrated luminosity	0.2
pileup	0.5
simulation statistics	0.5
$f_{correct}$	0.5
model calibration	0.2
selection efficiency	0.1
Theoretical uncertainties:	
top-quark mass	0.9
top-quark p_T	0.5
ME-PS	0.5
μ_R/μ_F	0.5
signal generator	0.5
underlying event	0.1
colour reconnection	0.1
hadronisation	0.5
PDF	0.1
t → Wq flavour	0.4
$|V_{td}|/|V_{ts}|$	<0.01
relative single-top-quark fraction (tW)	0.1
VV (theoretical cross section)	0.1
extra sources of heavy flavour	0.4
Total systematic	3.2

for the statistical uncertainties and Gaussian distributions for the systematic uncertainties. By constraining $|V_{tb}| \leq 1$, a similar procedure is used to obtain $|V_{tb}| > 0.975$ at the 95% CL.

6.4   Indirect measurement of the top-quark total decay width

The result obtained for $\mathcal{R}$ can be combined with a measurement of the single-top-quark production cross section in the t-channel to yield an indirect determination of the top-quark total width Γ_t. Assuming that $\sum_q \mathcal{B}(t \to Wq) = 1$, then $\mathcal{R} = \mathcal{B}(t \to Wb)$ and

$$\Gamma_t = \frac{\sigma_{t\text{-ch.}}}{\mathcal{B}(t \to Wb)} \cdot \frac{\Gamma(t \to Wb)}{\sigma_{t\text{-ch.}}^{\text{theor.}}}, \tag{7}$$

where $\sigma_{t\text{-ch.}}$ ($\sigma_{t\text{-ch.}}^{\text{theor.}}$) is the measured (theoretical) t-channel single-top-quark cross section and $\Gamma(t \to Wb)$ is the top-quark partial decay width to Wb. If we assume a top-quark mass of 172.5 GeV, then the theoretical partial width of the top quark decaying to Wb is $\Gamma(t \to Wb) = 1.329$ GeV [3]. A fit to the b-tagged jet multiplicity distribution in the data is performed, leaving Γ_t as a free parameter. In the likelihood function we use the theoretical prediction for the t-channel cross section at $\sqrt{s} = 7$ TeV from Ref. [56] and the corresponding
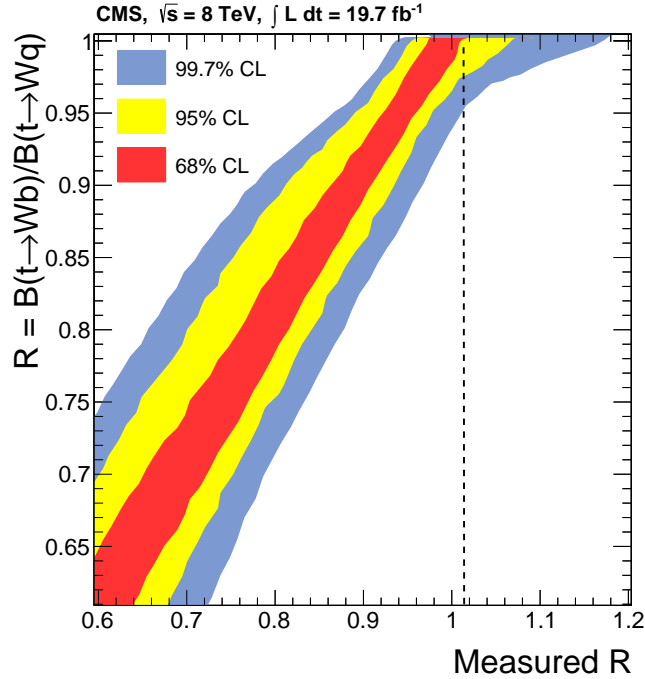
Figure 7: Expected limit bands at different confidence levels as a function of the measured $\mathcal{R}$ value. The range of measured values of $\mathcal{R}$ that are allowed for each true value of $\mathcal{R}$ are shown as coloured bands for different confidence levels. The observed value of $\mathcal{R}$ is shown as the dashed line.

CMS measurement from Ref. [24]. The uncertainties in the predicted and measured cross sections are taken into account as extra nuisance parameters in the fit. The uncertainty in the theoretical cross section is parameterised by convolving a Gaussian function for the PDF uncertainty with a uniform prior describing the factorisation and renormalisation scale uncertainties. Some uncertainties in the experimental cross section measurement such as those from JES and JER, b-tagging efficiency, μ_R/μ_F scales, and ME-PS threshold for $t\bar{t}$ production are fully correlated with the ones assigned to the measurement of $\mathcal{R}$. All others are summed in quadrature and assumed to be uncorrelated. After performing the maximum-likelihood fit, we measure $\Gamma_t = 1.36 \pm 0.02\,\text{(stat.)}^{+0.14}_{-0.11}\,\text{(syst.)}\,\text{GeV}$, in good agreement with the theoretical expectation [3]. The dominant uncertainty comes from the measurement of the t-channel cross section, as summarized in Table 5.

Table 5: Summary of the systematic uncertainties in the measurement of Γ_t. The values of the uncertainties are relative to the value of Γ_t obtained from the fit. The "Other sources" category combines all the individual contributions below 0.5%.

Source	Uncertainty (%)
Single-top quark t-channel cross section	9.2
ε_b	4.3
JES	0.7
pileup	0.8
ME-PS	0.8
μ_R/μ_F	0.8
top-quark mass	0.6
Other sources	1.5
Total systematic	10.4

7   Summary

A measurement of the ratio of the top-quark branching fractions $\mathcal{R} = \mathcal{B}(\text{t} \to \text{Wb})/\mathcal{B}(\text{t} \to \text{Wq})$, where the denominator includes the sum over the branching fractions of the top quark to a W boson and a down-type quark (q = b, s, d), has been performed using a sample of $\text{t}\bar{\text{t}}$ dilepton events. The sample has been selected from proton-proton collision data at $\sqrt{s} = 8\,\text{TeV}$ from an integrated luminosity of $19.7\,\text{fb}^{-1}$, collected with the CMS detector. The b-tagging and misidentification efficiencies are derived from multijet control samples. The fractions of events with 0, 1, or 2 selected jets from top-quark decays are determined using the lepton-jet invariant-mass spectrum and an empirical model for the misassignment contribution. The unconstrained measured value of $\mathcal{R} = 1.014 \pm 0.003\,(\text{stat.}) \pm 0.032\,(\text{syst.})$ is consistent with the SM prediction, and the main systematic uncertainty is from the b-tagging efficiency ($\approx 2.4\%$). All other uncertainties are $< 1\%$. A lower limit of $\mathcal{R} > 0.955$ at 95% CL is obtained after requiring $\mathcal{R} \leq 1$ and taking into account both statistical and systematical uncertainties. This result translates into a lower limit $|V_{\text{tb}}| > 0.975$ at 95% CL when assuming the unitarity of the three-generation CKM matrix. By combining this result with a previous CMS measurement of the t-channel production cross section for single top quarks, an indirect measurement of the top-quark total decay width $\Gamma_{\text{t}} = 1.36 \pm 0.02\,(\text{stat.})^{+0.14}_{-0.11}\,(\text{syst.})\,\text{GeV}$ is obtained, in agreement with the SM expectation. These measurements of $\mathcal{R}$ and Γ_{t} are the most precise to date and the first obtained at the LHC.

Acknowledgements

References

[1] CDF and D0 Collaborations, "Combination of the top quark mass measurements from the Tevatron collider", *Phys. Rev. D* **86** (2012) 092003, `doi:10.1103/PhysRevD.86.092003`, `arXiv:1207.1069`.

[2] I. I. Bigi, "Weak decays of heavy flavors: a phenomenological update", *Phys. Lett. B* **169** (1986) 101, `doi:10.1016/0370-2693(86)90694-5`.

[3] Particle Data Group, J. Beringer et al., "Review of Particle Physics", *Phys. Rev. D* **86** (2012) 010001, `doi:10.1103/PhysRevD.86.010001`.

[4] J. Alwall et al., "Is $V_{tb} \simeq 1$?", *Eur. Phys. J. C* **49** (2007) 791, `doi:10.1140/epjc/s10052-006-0137-y`, `arXiv:hep-ph/0607115`.

[5] CMS Collaboration, "Search for heavy bottom-like quarks in $4.9\,\text{fb}^{-1}$ of pp collisions at $\sqrt{s} = 7\,\text{TeV}$", *JHEP* **05** (2012) 123, `doi:10.1007/JHEP05(2012)123`, `arXiv:1204.1088`.

[6] CMS Collaboration, "Combined search for the quarks of a sequential fourth generation", *Phys. Rev. D* **86** (2012) 112003, `doi:10.1103/PhysRevD.86.112003`, `arXiv:1209.1062`.

[7] ATLAS Collaboration, "Search for pair-produced heavy quarks decaying to Wq in the two-lepton channel at $\sqrt{s} = 7\,\text{TeV}$ with the ATLAS detector", *Phys. Rev. D* **86** (2012) 012007, `doi:10.1103/PhysRevD.86.012007`, `arXiv:1202.3389`.

[8] CMS Collaboration, "Search for heavy, top-like quark pair production in the dilepton final state in pp collisions at $\sqrt{s} = 7\,\text{TeV}$", *Phys. Lett. B* **716** (2012) 103, `doi:10.1016/j.physletb.2012.07.059`, `arXiv:1203.5410`.

[9] ATLAS Collaboration, "Search for pair production of heavy top-like quarks decaying to a high-p_T W boson and a b quark in the lepton plus jets final state at $\sqrt{s}$=7 TeV with the ATLAS detector", *Phys. Lett. B* **718** (2013) 1284, `doi:10.1016/j.physletb.2012.11.071`, `arXiv:1210.5468`.

[10] ATLAS Collaboration, "Search for pair production of a new quark that decays to a Z boson and a bottom quark with the ATLAS detector", *Phys. Rev. Lett.* **109** (2012) 071801, `doi:10.1103/PhysRevLett.109.071801`, `arXiv:1204.1265`.

[11] CMS Collaboration, "Inclusive search for a vector-like T quark with charge 2/3 in pp collisions at $\sqrt{s} = 8\,\text{TeV}$", *Phys. Lett. B* **729** (2014) 149, `doi:10.1016/j.physletb.2014.01.006`, `arXiv:1311.7667`.

[12] CMS Collaboration, "Search for top-quark partners with charge 5/3 in the same-sign dilepton final state", (2013). `arXiv:1312.2391`. Submitted to Phys. Rev. Lett.

[13] CMS Collaboration, "Search for a light charged Higgs boson in top quark decays in pp collisions at $\sqrt{s} = 7\,\text{TeV}$", *JHEP* **07** (2012) 143, `doi:10.1007/JHEP07(2012)143`, `arXiv:1205.5736`.

[14] ATLAS Collaboration, "Search for a light charged Higgs boson in the decay channel $H^+ \to c\bar{s}$ in $t\bar{t}$ events using pp collisions at $\sqrt{s}$ = 7 TeV with the ATLAS detector", *Eur. Phys. J. C* **73** (2013) 2465, `doi:10.1140/epjc/s10052-013-2465-z`, `arXiv:1302.3694`.

[15] ATLAS Collaboration, "Search for charged Higgs bosons through the violation of lepton universality in $t\bar{t}$ events using pp collision data at $\sqrt{s} = 7$ TeV with the ATLAS experiment", *JHEP* **03** (2013) 076, `doi:10.1007/JHEP03(2013)076`, `arXiv:1212.3572`.

[16] ATLAS Collaboration, "Observation of a new particle in the search for the Standard Model Higgs boson with the ATLAS detector at the LHC", *Phys. Lett. B* **716** (2012) 1, `doi:10.1016/j.physletb.2012.08.020`, `arXiv:1207.7214`.

[17] CMS Collaboration, "Observation of a new boson at a mass of 125 GeV with the CMS experiment at the LHC", *Phys. Lett. B* **716** (2012) 30, `doi:10.1016/j.physletb.2012.08.021`, `arXiv:1207.7235`.

[18] CMS Collaboration, "Observation of a new boson with mass near 125 GeV in pp collisions at $\sqrt{s}$ = 7 and 8 TeV", *JHEP* **06** (2013) 081, `doi:10.1007/JHEP06(2013)081`, `arXiv:1303.4571`.

[19] C. P. Yuan, "A new method to detect a heavy top quark at the Tevatron", *Phys. Rev. D* **41** (1990) 42, `doi:10.1103/PhysRevD.41.42`.

[20] D0 Collaboration, "An improved determination of the width of the top quark", *Phys. Rev. D* **85** (2012) 091104, `doi:10.1103/PhysRevD.85.091104`, `arXiv:1201.4156`.

[21] D0 Collaboration, "Precision measurement of the ratio $\mathcal{B}(t \to Wb)/\mathcal{B}(t \to Wq)$", *Phys. Rev. Lett.* **107** (2011) 121802, `doi:10.1103/PhysRevLett.107.121802`, `arXiv:1106.5436`.

[22] CDF Collaboration, "Measurement of $R = \mathcal{B}(t \to Wb)/\mathcal{B}(t \to Wq)$ in top quark pair decays using lepton+jets events and the full CDF Run II data set", *Phys. Rev. D* **87** (2013) 111101, `doi:10.1103/PhysRevD.87.111101`, `arXiv:1303.6142`.

[23] CMS Collaboration, "CMS luminosity based on pixel cluster counting - Summer 2013 Update", CMS Physics Analysis Summary CMS-PAS-LUM-13-001, 2013.

[24] CMS Collaboration, "Measurement of the single-top-quark *t*-channel cross section in pp collisions at $\sqrt{s} = 7$ TeV", *JHEP* **12** (2012) 035, `doi:10.1007/JHEP12(2012)035`, `arXiv:1209.4533`.

[25] CMS Collaboration, "Energy calibration and resolution of the CMS electromagnetic calorimeter in pp collisions at $\sqrt{s} = 7$ TeV", *JINST* **8** (2013) P09009, `doi:10.1088/1748-0221/8/09/P09009`, `arXiv:1306.2016`.

[26] CMS Collaboration, "Determination of jet energy calibration and transverse momentum resolution in CMS", *JINST* **6** (2011) P11002, `doi:10.1088/1748-0221/6/11/P11002`, `arXiv:1107.4277`.

[27] CMS Collaboration, "The CMS experiment at the CERN LHC", *JINST* **3** (2008) S08004, `doi:10.1088/1748-0221/3/08/S08004`.

[28] M. Czakon, P. Fiedler, and A. Mitov, "The total top quark pair production cross section at hadron colliders through $\mathcal{O}(\alpha_S^4)$", *Phys. Rev. Lett.* **110** (2013) 252004, `doi:10.1103/PhysRevLett.110.252004`, `arXiv:1303.6254`.

[29] J. Alwall et al., "MadGraph 5: going beyond", *JHEP* **06** (2011) 128, `doi:10.1007/JHEP06(2011)128`, `arXiv:1106.0522`.

[30] T. Sjöstrand, S. Mrenna, and P. Z. Skands, "PYTHIA 6.4 physics and manual", *JHEP* **05** (2006) 026, `doi:10.1088/1126-6708/2006/05/026`, `arXiv:hep-ph/0603175`.

[31] N. Davidson et al., "Universal interface of TAUOLA technical and physics documentation", *Comput. Phys. Commun.* **183** (2012) 821, `doi:10.1016/j.cpc.2011.12.009`, `arXiv:1002.0543`.

[32] J. Pumplin et al., "New generation of parton distributions with uncertainties from global QCD analysis", *JHEP* **07** (2002) 012, `doi:10.1088/1126-6708/2002/07/012`, `arXiv:hep-ph/0201195`.

[33] N. Kidonakis, "Differential and total cross sections for top pair and single top production", in *XX International Workshop on Deep-Inelastic Scattering and Related Subjects*, p. 831. 2012. `arXiv:1205.3453`. An update can be found in `arXiv:1311.0283`. `doi:10.3204/DESY-PROC-2012-02/251`.

[34] K. Melnikov and F. Petriello, "Electroweak gauge boson production at hadron colliders through $\mathcal{O}(\alpha_S^2)$", *Phys. Rev. D* **74** (2006) 114017, `doi:10.1103/PhysRevD.74.114017`, `arXiv:hep-ph/0609070`.

[35] P. Nason, "A new method for combining NLO QCD with shower Monte Carlo algorithms", *JHEP* **11** (2004) 040, `doi:10.1088/1126-6708/2004/11/040`, `arXiv:hep-ph/0409146`.

[36] S. Frixione, P. Nason, and C. Oleari, "Matching NLO QCD computations with parton shower simulations: the POWHEG method", *JHEP* **11** (2007) 070, `doi:10.1088/1126-6708/2007/11/070`, `arXiv:0709.2092`.

[37] S. Alioli, P. Nason, C. Oleari, and E. Re, "A general framework for implementing NLO calculations in shower Monte Carlo programs: the POWHEG BOX", *JHEP* **06** (2010) 043, `doi:10.1007/JHEP06(2010)043`, `arXiv:1002.2581`.

[38] S. Alioli, P. Nason, C. Oleari, and E. Re, "NLO single-top production matched with shower in POWHEG: *s*- and *t*-channel contributions", *JHEP* **09** (2009) 111, `doi:10.1088/1126-6708/2009/09/111`, `arXiv:0907.4076`. [Erratum: `doi:10.1007/JHEP02(2010)011`].

[39] E. Re, "Single-top *Wt*-channel production matched with parton showers using the POWHEG method", *Eur. Phys. J. C* **71** (2011) 1547, `doi:10.1140/epjc/s10052-011-1547-z`, `arXiv:1009.2450`.

[40] J. M. Campbell and R. K. Ellis, "MCFM for the Tevatron and the LHC", *Nucl. Phys. Proc. Suppl.* **205** (2010) 10, `doi:10.1016/j.nuclphysbps.2010.08.011`, `arXiv:1007.3492`.

[41] J. Allison et al., "GEANT4 developments and applications", *IEEE Trans. Nucl. Sci.* **53** (2006) 270, `doi:10.1109/TNS.2006.869826`.

[42] GEANT4 Collaboration, "GEANT4—a simulation toolkit", *Nucl. Instrum. Meth. A* **506** (2003) 250, `doi:10.1016/S0168-9002(03)01368-8`.

[43] CMS Collaboration, "Particle flow event reconstruction in CMS and performance for jets, taus, and E_T^{miss}", CMS Physics Analysis Summary CMS-PAS-PFT-09-001, 2009.

[44] CMS Collaboration, "Commissioning of the particle flow event reconstruction with the first LHC collisions recorded in the CMS detector", CMS Physics Analysis Summary CMS-PAS-PFT-10-001, 2010.

[45] M. Cacciari, G. P. Salam, and G. Soyez, "The anti-k_t jet clustering algorithm", *JHEP* **04** (2008) 063, `doi:10.1088/1126-6708/2008/04/063`, `arXiv:0802.1189`.

[46] M. Cacciari, G. P. Salam, and G. Soyez, "The catchment area of jets", *JHEP* **04** (2008) 005, `doi:10.1088/1126-6708/2008/04/05`, `arXiv:0802.1188`.

[47] M. Cacciari and G. P. Salam, "Pileup subtraction using jet areas", *Phys. Lett. B* **659** (2008) 119, `doi:10.1016/j.physletb.2007.09.077`, `arXiv:0707.1378`.

[48] G. Cowan, K. Cranmer, E. Gross, and O. Vitells, "Asymptotic formulae for likelihood-based tests of new physics", *Eur. Phys. J. C* **71** (2011) 1554, `doi:10.1140/epjc/s10052-011-1554-0`, `arXiv:1007.1727`.

[49] CMS Collaboration, "Measurement of the $t\bar{t}$ production cross section in the dilepton channel in pp collisions at $\sqrt{s} = 8$ TeV", *JHEP* **02** (2014) 024, `doi:10.1007/JHEP02(2014)024`, `arXiv:1312.7582`.

[50] CMS Collaboration, "Identification of b-quark jets with the CMS experiment", *JINST* **8** (2013) P04013, `doi:10.1088/1748-0221/8/04/P04013`, `arXiv:1211.4462`.

[51] CMS Collaboration, "Performance of b tagging at $\sqrt{s} = 8$ TeV in multijet, $t\bar{t}$ and boosted topology events", CMS Physics Analysis Summary CMS-PAS-BTV-13-001, 2012.

[52] R. K. Ellis, W. J. Stirling, and B. R. Webber, "QCD and collider physics". Cambridge University Press, 1996.

[53] P. Silva and M. Gallinaro, "Probing the flavor of the top quark decay", *Nuovo Cim. B* **125** (2010) 983, `doi:10.1393/ncb/i2010-10896-0`, `arXiv:1010.2994`.

[54] G. J. Feldman and R. D. Cousins, "A unified approach to the classical statistical analysis of small signals", *Phys. Rev. D* **57** (1998) 3873, `doi:10.1103/PhysRevD.57.3873`, `arXiv:physics/9711021`.

[55] L. Moneta et al., "The RooStats Project", in *13th International Workshop on Advanced Computing and Analysis Techniques in Physics Research (ACAT2010)*. SISSA, 2010. `arXiv:1009.1003`. PoS(ACAT2010)057.

[56] N. Kidonakis, "Next-to-next-to-leading-order collinear and soft gluon corrections for *t*-channel single top quark production", *Phys. Rev. D* **83** (2011) 091503, `doi:10.1103/PhysRevD.83.091503`, `arXiv:1103.2792`.

A   The CMS Collaboration

Yerevan Physics Institute, Yerevan, Armenia
V. Khachatryan, A.M. Sirunyan, A. Tumasyan

Institut für Hochenergiephysik der OeAW, Wien, Austria
W. Adam, T. Bergauer, M. Dragicevic, J. Erö, C. Fabjan[1], M. Friedl, R. Frühwirth[1], V.M. Ghete, C. Hartl, N. Hörmann, J. Hrubec, M. Jeitler[1], W. Kiesenhofer, V. Knünz, M. Krammer[1], I. Krätschmer, D. Liko, I. Mikulec, D. Rabady[2], B. Rahbaran, H. Rohringer, R. Schöfbeck, J. Strauss, A. Taurok, W. Treberer-Treberspurg, W. Waltenberger, C.-E. Wulz[1]

National Centre for Particle and High Energy Physics, Minsk, Belarus
V. Mossolov, N. Shumeiko, J. Suarez Gonzalez

Universiteit Antwerpen, Antwerpen, Belgium
S. Alderweireldt, M. Bansal, S. Bansal, T. Cornelis, E.A. De Wolf, X. Janssen, A. Knutsson, S. Luyckx, S. Ochesanu, B. Roland, R. Rougny, M. Van De Klundert, H. Van Haevermaet, P. Van Mechelen, N. Van Remortel, A. Van Spilbeeck

Vrije Universiteit Brussel, Brussel, Belgium
F. Blekman, S. Blyweert, J. D'Hondt, N. Daci, N. Heracleous, A. Kalogeropoulos, J. Keaveney, T.J. Kim, S. Lowette, M. Maes, A. Olbrechts, Q. Python, D. Strom, S. Tavernier, W. Van Doninck, P. Van Mulders, G.P. Van Onsem, I. Villella

Université Libre de Bruxelles, Bruxelles, Belgium
C. Caillol, B. Clerbaux, G. De Lentdecker, L. Favart, A.P.R. Gay, A. Grebenyuk, A. Léonard, P.E. Marage, A. Mohammadi, L. Perniè, T. Reis, T. Seva, L. Thomas, C. Vander Velde, P. Vanlaer, J. Wang

Ghent University, Ghent, Belgium
V. Adler, K. Beernaert, L. Benucci, A. Cimmino, S. Costantini, S. Crucy, S. Dildick, A. Fagot, G. Garcia, B. Klein, J. Mccartin, A.A. Ocampo Rios, D. Ryckbosch, S. Salva Diblen, M. Sigamani, N. Strobbe, F. Thyssen, M. Tytgat, E. Yazgan, N. Zaganidis

Université Catholique de Louvain, Louvain-la-Neuve, Belgium
S. Basegmez, C. Beluffi[3], G. Bruno, R. Castello, A. Caudron, L. Ceard, G.G. Da Silveira, C. Delaere, T. du Pree, D. Favart, L. Forthomme, A. Giammanco[4], J. Hollar, P. Jez, M. Komm, V. Lemaitre, J. Liao, C. Nuttens, D. Pagano, A. Pin, K. Piotrzkowski, A. Popov[5], L. Quertenmont, M. Selvaggi, M. Vidal Marono, J.M. Vizan Garcia

Université de Mons, Mons, Belgium
N. Beliy, T. Caebergs, E. Daubie, G.H. Hammad

Centro Brasileiro de Pesquisas Fisicas, Rio de Janeiro, Brazil
G.A. Alves, M. Correa Martins Junior, T. Dos Reis Martins, M.E. Pol

Universidade do Estado do Rio de Janeiro, Rio de Janeiro, Brazil
W.L. Aldá Júnior, W. Carvalho, J. Chinellato[6], A. Custódio, E.M. Da Costa, D. De Jesus Damiao, C. De Oliveira Martins, S. Fonseca De Souza, H. Malbouisson, M. Malek, D. Matos Figueiredo, L. Mundim, H. Nogima, W.L. Prado Da Silva, J. Santaolalla, A. Santoro, A. Sznajder, E.J. Tonelli Manganote[6], A. Vilela Pereira

Universidade Estadual Paulista [a]**, Universidade Federal do ABC** [b]**, São Paulo, Brazil**
C.A. Bernardes[b], F.A. Dias[a,7], T.R. Fernandez Perez Tomei[a], E.M. Gregores[b], P.G. Mercadante[b], S.F. Novaes[a], Sandra S. Padula[a]

Institute for Nuclear Research and Nuclear Energy, Sofia, Bulgaria
V. Genchev[2], P. Iaydjiev[2], A. Marinov, S. Piperov, M. Rodozov, G. Sultanov, M. Vutova

University of Sofia, Sofia, Bulgaria
A. Dimitrov, I. Glushkov, R. Hadjiiska, V. Kozhuharov, L. Litov, B. Pavlov, P. Petkov

Institute of High Energy Physics, Beijing, China
J.G. Bian, G.M. Chen, H.S. Chen, M. Chen, R. Du, C.H. Jiang, D. Liang, S. Liang, R. Plestina[8], J. Tao, X. Wang, Z. Wang

State Key Laboratory of Nuclear Physics and Technology, Peking University, Beijing, China
C. Asawatangtrakuldee, Y. Ban, Y. Guo, Q. Li, W. Li, S. Liu, Y. Mao, S.J. Qian, D. Wang, L. Zhang, W. Zou

Universidad de Los Andes, Bogota, Colombia
C. Avila, L.F. Chaparro Sierra, C. Florez, J.P. Gomez, B. Gomez Moreno, J.C. Sanabria

Technical University of Split, Split, Croatia
N. Godinovic, D. Lelas, D. Polic, I. Puljak

University of Split, Split, Croatia
Z. Antunovic, M. Kovac

Institute Rudjer Boskovic, Zagreb, Croatia
V. Brigljevic, K. Kadija, J. Luetic, D. Mekterovic, S. Morovic, L. Sudic

University of Cyprus, Nicosia, Cyprus
A. Attikis, G. Mavromanolakis, J. Mousa, C. Nicolaou, F. Ptochos, P.A. Razis

Charles University, Prague, Czech Republic
M. Bodlak, M. Finger, M. Finger Jr.

Academy of Scientific Research and Technology of the Arab Republic of Egypt, Egyptian Network of High Energy Physics, Cairo, Egypt
Y. Assran[9], A. Ellithi Kamel[10], M.A. Mahmoud[11], A. Radi[12,13]

National Institute of Chemical Physics and Biophysics, Tallinn, Estonia
M. Kadastik, M. Murumaa, M. Raidal, A. Tiko

Department of Physics, University of Helsinki, Helsinki, Finland
P. Eerola, G. Fedi, M. Voutilainen

Helsinki Institute of Physics, Helsinki, Finland
J. Härkönen, V. Karimäki, R. Kinnunen, M.J. Kortelainen, T. Lampén, K. Lassila-Perini, S. Lehti, T. Lindén, P. Luukka, T. Mäenpää, T. Peltola, E. Tuominen, J. Tuominiemi, E. Tuovinen, L. Wendland

Lappeenranta University of Technology, Lappeenranta, Finland
T. Tuuva

DSM/IRFU, CEA/Saclay, Gif-sur-Yvette, France
M. Besancon, F. Couderc, M. Dejardin, D. Denegri, B. Fabbro, J.L. Faure, C. Favaro, F. Ferri, S. Ganjour, A. Givernaud, P. Gras, G. Hamel de Monchenault, P. Jarry, E. Locci, J. Malcles, A. Nayak, J. Rander, A. Rosowsky, M. Titov

Laboratoire Leprince-Ringuet, Ecole Polytechnique, IN2P3-CNRS, Palaiseau, France
S. Baffioni, F. Beaudette, P. Busson, C. Charlot, T. Dahms, M. Dalchenko, L. Dobrzynski,

N. Filipovic, A. Florent, R. Granier de Cassagnac, L. Mastrolorenzo, P. Miné, C. Mironov, I.N. Naranjo, M. Nguyen, C. Ochando, P. Paganini, R. Salerno, J.b. Sauvan, Y. Sirois, C. Veelken, Y. Yilmaz, A. Zabi

Institut Pluridisciplinaire Hubert Curien, Université de Strasbourg, Université de Haute Alsace Mulhouse, CNRS/IN2P3, Strasbourg, France
J.-L. Agram[14], J. Andrea, A. Aubin, D. Bloch, J.-M. Brom, E.C. Chabert, C. Collard, E. Conte[14], J.-C. Fontaine[14], D. Gelé, U. Goerlach, C. Goetzmann, A.-C. Le Bihan, P. Van Hove

Centre de Calcul de l'Institut National de Physique Nucleaire et de Physique des Particules, CNRS/IN2P3, Villeurbanne, France
S. Gadrat

Université de Lyon, Université Claude Bernard Lyon 1, CNRS-IN2P3, Institut de Physique Nucléaire de Lyon, Villeurbanne, France
S. Beauceron, N. Beaupere, G. Boudoul, S. Brochet, C.A. Carrillo Montoya, J. Chasserat, R. Chierici, D. Contardo[2], P. Depasse, H. El Mamouni, J. Fan, J. Fay, S. Gascon, M. Gouzevitch, B. Ille, T. Kurca, M. Lethuillier, L. Mirabito, S. Perries, J.D. Ruiz Alvarez, D. Sabes, L. Sgandurra, V. Sordini, M. Vander Donckt, P. Verdier, S. Viret, H. Xiao

Institute of High Energy Physics and Informatization, Tbilisi State University, Tbilisi, Georgia
Z. Tsamalaidze[15]

RWTH Aachen University, I. Physikalisches Institut, Aachen, Germany
C. Autermann, S. Beranek, M. Bontenackels, B. Calpas, M. Edelhoff, L. Feld, O. Hindrichs, K. Klein, A. Ostapchuk, A. Perieanu, F. Raupach, J. Sammet, S. Schael, D. Sprenger, H. Weber, B. Wittmer, V. Zhukov[5]

RWTH Aachen University, III. Physikalisches Institut A, Aachen, Germany
M. Ata, J. Caudron, E. Dietz-Laursonn, D. Duchardt, M. Erdmann, R. Fischer, A. Güth, T. Hebbeker, C. Heidemann, K. Hoepfner, D. Klingebiel, S. Knutzen, P. Kreuzer, M. Merschmeyer, A. Meyer, M. Olschewski, K. Padeken, P. Papacz, H. Reithler, S.A. Schmitz, L. Sonnenschein, D. Teyssier, S. Thüer, M. Weber

RWTH Aachen University, III. Physikalisches Institut B, Aachen, Germany
V. Cherepanov, Y. Erdogan, G. Flügge, H. Geenen, M. Geisler, W. Haj Ahmad, F. Hoehle, B. Kargoll, T. Kress, Y. Kuessel, J. Lingemann[2], A. Nowack, I.M. Nugent, L. Perchalla, O. Pooth, A. Stahl

Deutsches Elektronen-Synchrotron, Hamburg, Germany
I. Asin, N. Bartosik, J. Behr, W. Behrenhoff, U. Behrens, A.J. Bell, M. Bergholz[16], A. Bethani, K. Borras, A. Burgmeier, A. Cakir, L. Calligaris, A. Campbell, S. Choudhury, F. Costanza, C. Diez Pardos, S. Dooling, T. Dorland, G. Eckerlin, D. Eckstein, T. Eichhorn, G. Flucke, J. Garay Garcia, A. Geiser, P. Gunnellini, J. Hauk, G. Hellwig, M. Hempel, D. Horton, H. Jung, M. Kasemann, P. Katsas, J. Kieseler, C. Kleinwort, D. Krücker, W. Lange, J. Leonard, K. Lipka, W. Lohmann[16], B. Lutz, R. Mankel, I. Marfin, I.-A. Melzer-Pellmann, A.B. Meyer, J. Mnich, A. Mussgiller, S. Naumann-Emme, O. Novgorodova, F. Nowak, E. Ntomari, H. Perrey, D. Pitzl, R. Placakyte, A. Raspereza, P.M. Ribeiro Cipriano, E. Ron, M.Ö. Sahin, J. Salfeld-Nebgen, P. Saxena, R. Schmidt[16], T. Schoerner-Sadenius, M. Schröder, A.D.R. Vargas Trevino, R. Walsh, C. Wissing

University of Hamburg, Hamburg, Germany
M. Aldaya Martin, V. Blobel, M. Centis Vignali, J. Erfle, E. Garutti, K. Goebel, M. Görner,

M. Gosselink, J. Haller, R.S. Höing, H. Kirschenmann, R. Klanner, R. Kogler, J. Lange, T. Lapsien, T. Lenz, I. Marchesini, J. Ott, T. Peiffer, N. Pietsch, D. Rathjens, C. Sander, H. Schettler, P. Schleper, E. Schlieckau, A. Schmidt, M. Seidel, J. Sibille[17], V. Sola, H. Stadie, G. Steinbrück, D. Troendle, E. Usai, L. Vanelderen

Institut für Experimentelle Kernphysik, Karlsruhe, Germany
C. Barth, C. Baus, J. Berger, C. Böser, E. Butz, T. Chwalek, W. De Boer, A. Descroix, A. Dierlamm, M. Feindt, M. Guthoff[2], F. Hartmann[2], T. Hauth[2], U. Husemann, I. Katkov[5], A. Kornmayer[2], E. Kuznetsova, P. Lobelle Pardo, M.U. Mozer, Th. Müller, A. Nürnberg, G. Quast, K. Rabbertz, F. Ratnikov, S. Röcker, H.J. Simonis, F.M. Stober, R. Ulrich, J. Wagner-Kuhr, S. Wayand, T. Weiler

Institute of Nuclear and Particle Physics (INPP),   NCSR Demokritos, Aghia Paraskevi, Greece
G. Anagnostou, G. Daskalakis, T. Geralis, V.A. Giakoumopoulou, A. Kyriakis, D. Loukas, A. Markou, C. Markou, A. Psallidas, I. Topsis-Giotis

University of Athens, Athens, Greece
L. Gouskos, A. Panagiotou, N. Saoulidou, E. Stiliaris

University of Ioánnina, Ioánnina, Greece
X. Aslanoglou, I. Evangelou[2], G. Flouris, C. Foudas[2], P. Kokkas, N. Manthos, I. Papadopoulos, E. Paradas

Wigner Research Centre for Physics, Budapest, Hungary
G. Bencze[2], C. Hajdu, P. Hidas, D. Horvath[18], F. Sikler, V. Veszpremi, G. Vesztergombi[19], A.J. Zsigmond

Institute of Nuclear Research ATOMKI, Debrecen, Hungary
N. Beni, S. Czellar, J. Karancsi[20], J. Molnar, J. Palinkas, Z. Szillasi

University of Debrecen, Debrecen, Hungary
P. Raics, Z.L. Trocsanyi, B. Ujvari

National Institute of Science Education and Research, Bhubaneswar, India
S.K. Swain

Panjab University, Chandigarh, India
S.B. Beri, V. Bhatnagar, N. Dhingra, R. Gupta, A.K. Kalsi, M. Kaur, M. Mittal, N. Nishu, J.B. Singh

University of Delhi, Delhi, India
Ashok Kumar, Arun Kumar, S. Ahuja, A. Bhardwaj, B.C. Choudhary, A. Kumar, S. Malhotra, M. Naimuddin, K. Ranjan, V. Sharma

Saha Institute of Nuclear Physics, Kolkata, India
S. Banerjee, S. Bhattacharya, K. Chatterjee, S. Dutta, B. Gomber, Sa. Jain, Sh. Jain, R. Khurana, A. Modak, S. Mukherjee, D. Roy, S. Sarkar, M. Sharan

Bhabha Atomic Research Centre, Mumbai, India
A. Abdulsalam, D. Dutta, S. Kailas, V. Kumar, A.K. Mohanty[2], L.M. Pant, P. Shukla, A. Topkar

Tata Institute of Fundamental Research - EHEP, Mumbai, India
T. Aziz, R.M. Chatterjee, S. Ganguly, S. Ghosh, M. Guchait[21], A. Gurtu[22], G. Kole, S. Kumar, M. Maity[23], G. Majumder, K. Mazumdar, G.B. Mohanty, B. Parida, K. Sudhakar, N. Wickramage[24]

Tata Institute of Fundamental Research - HECR, Mumbai, India
S. Banerjee, R.K. Dewanjee, S. Dugad

Institute for Research in Fundamental Sciences (IPM), Tehran, Iran
H. Bakhshiansohi, H. Behnamian, S.M. Etesami[25], A. Fahim[26], A. Jafari, M. Khakzad, M. Mohammadi Najafabadi, M. Naseri, S. Paktinat Mehdiabadi, B. Safarzadeh[27], M. Zeinali

University College Dublin, Dublin, Ireland
M. Felcini, M. Grunewald

INFN Sezione di Bari [a], Università di Bari [b], Politecnico di Bari [c], Bari, Italy
M. Abbrescia[a,b], L. Barbone[a,b], C. Calabria[a,b], S.S. Chhibra[a,b], A. Colaleo[a], D. Creanza[a,c], N. De Filippis[a,c], M. De Palma[a,b], L. Fiore[a], G. Iaselli[a,c], G. Maggi[a,c], M. Maggi[a], S. My[a,c], S. Nuzzo[a,b], N. Pacifico[a], A. Pompili[a,b], G. Pugliese[a,c], R. Radogna[a,b], G. Selvaggi[a,b], L. Silvestris[a], G. Singh[a,b], R. Venditti[a,b], P. Verwilligen[a], G. Zito[a]

INFN Sezione di Bologna [a], Università di Bologna [b], Bologna, Italy
G. Abbiendi[a], A.C. Benvenuti[a], D. Bonacorsi[a,b], S. Braibant-Giacomelli[a,b], L. Brigliadori[a,b], R. Campanini[a,b], P. Capiluppi[a,b], A. Castro[a,b], F.R. Cavallo[a], G. Codispoti[a,b], M. Cuffiani[a,b], G.M. Dallavalle[a], F. Fabbri[a], A. Fanfani[a,b], D. Fasanella[a,b], P. Giacomelli[a], C. Grandi[a], L. Guiducci[a,b], S. Marcellini[a], G. Masetti[a], A. Montanari[a], F.L. Navarria[a,b], A. Perrotta[a], F. Primavera[a,b], A.M. Rossi[a,b], T. Rovelli[a,b], G.P. Siroli[a,b], N. Tosi[a,b], R. Travaglini[a,b]

INFN Sezione di Catania [a], Università di Catania [b], CSFNSM [c], Catania, Italy
S. Albergo[a,b], G. Cappello[a], M. Chiorboli[a,b], S. Costa[a,b], F. Giordano[a,2], R. Potenza[a,b], A. Tricomi[a,b], C. Tuve[a,b]

INFN Sezione di Firenze [a], Università di Firenze [b], Firenze, Italy
G. Barbagli[a], V. Ciulli[a,b], C. Civinini[a], R. D'Alessandro[a,b], E. Focardi[a,b], E. Gallo[a], S. Gonzi[a,b], V. Gori[a,b], P. Lenzi[a,b], M. Meschini[a], S. Paoletti[a], G. Sguazzoni[a], A. Tropiano[a,b]

INFN Laboratori Nazionali di Frascati, Frascati, Italy
L. Benussi, S. Bianco, F. Fabbri, D. Piccolo

INFN Sezione di Genova [a], Università di Genova [b], Genova, Italy
F. Ferro[a], M. Lo Vetere[a,b], E. Robutti[a], S. Tosi[a,b]

INFN Sezione di Milano-Bicocca [a], Università di Milano-Bicocca [b], Milano, Italy
M.E. Dinardo[a,b], S. Fiorendi[a,b,2], S. Gennai[a], R. Gerosa, A. Ghezzi[a,b], P. Govoni[a,b], M.T. Lucchini[a,b,2], S. Malvezzi[a], R.A. Manzoni[a,b,2], A. Martelli[a,b,2], B. Marzocchi, D. Menasce[a], L. Moroni[a], M. Paganoni[a,b], D. Pedrini[a], S. Ragazzi[a,b], N. Redaelli[a], T. Tabarelli de Fatis[a,b]

INFN Sezione di Napoli [a], Università di Napoli 'Federico II' [b], Università della Basilicata (Potenza) [c], Università G. Marconi (Roma) [d], Napoli, Italy
S. Buontempo[a], N. Cavallo[a,c], S. Di Guida[a,d], F. Fabozzi[a,c], A.O.M. Iorio[a,b], L. Lista[a], S. Meola[a,d,2], M. Merola[a], P. Paolucci[a,2]

INFN Sezione di Padova [a], Università di Padova [b], Università di Trento (Trento) [c], Padova, Italy
P. Azzi[a], N. Bacchetta[a], D. Bisello[a,b], A. Branca[a,b], R. Carlin[a,b], P. Checchia[a], T. Dorigo[a], U. Dosselli[a], M. Galanti[a,b], F. Gasparini[a,b], U. Gasparini[a,b], F. Gonella[a], A. Gozzelino[a], K. Kanishchev[a,c], S. Lacaprara[a], M. Margoni[a,b], A.T. Meneguzzo[a,b], J. Pazzini[a,b], N. Pozzobon[a,b], P. Ronchese[a,b], F. Simonetto[a,b], E. Torassa[a], M. Tosi[a,b], P. Zotto[a,b], A. Zucchetta[a,b], G. Zumerle[a,b]

INFN Sezione di Pavia [a]**, Università di Pavia** [b]**, Pavia, Italy**
M. Gabusi[a,b], S.P. Ratti[a,b], C. Riccardi[a,b], P. Salvini[a], P. Vitulo[a,b]

INFN Sezione di Perugia [a]**, Università di Perugia** [b]**, Perugia, Italy**
M. Biasini[a,b], G.M. Bilei[a], L. Fanò[a,b], P. Lariccia[a,b], G. Mantovani[a,b], M. Menichelli[a], F. Romeo[a,b], A. Saha[a], A. Santocchia[a,b], A. Spiezia[a,b]

INFN Sezione di Pisa [a]**, Università di Pisa** [b]**, Scuola Normale Superiore di Pisa** [c]**, Pisa, Italy**
K. Androsov[a,28], P. Azzurri[a], G. Bagliesi[a], J. Bernardini[a], T. Boccali[a], G. Broccolo[a,c], R. Castaldi[a], M.A. Ciocci[a,28], R. Dell'Orso[a], S. Donato[a,c], F. Fiori[a,c], L. Foà[a,c], A. Giassi[a], M.T. Grippo[a,28], F. Ligabue[a,c], T. Lomtadze[a], L. Martini[a,b], A. Messineo[a,b], C.S. Moon[a,29], F. Palla[a,2], A. Rizzi[a,b], A. Savoy-Navarro[a,30], A.T. Serban[a], P. Spagnolo[a], P. Squillacioti[a,28], R. Tenchini[a], G. Tonelli[a,b], A. Venturi[a], P.G. Verdini[a], C. Vernieri[a,c]

INFN Sezione di Roma [a]**, Università di Roma** [b]**, Roma, Italy**
L. Barone[a,b], F. Cavallari[a], D. Del Re[a,b], M. Diemoz[a], M. Grassi[a,b], C. Jorda[a], E. Longo[a,b], F. Margaroli[a,b], P. Meridiani[a], F. Micheli[a,b], S. Nourbakhsh[a,b], G. Organtini[a,b], R. Paramatti[a], S. Rahatlou[a,b], C. Rovelli[a], F. Santanastasio[a,b], L. Soffi[a,b], P. Traczyk[a,b]

INFN Sezione di Torino [a]**, Università di Torino** [b]**, Università del Piemonte Orientale (Novara)** [c]**, Torino, Italy**
N. Amapane[a,b], R. Arcidiacono[a,c], S. Argiro[a,b], M. Arneodo[a,c], R. Bellan[a,b], C. Biino[a], N. Cartiglia[a], S. Casasso[a,b], M. Costa[a,b], A. Degano[a,b], N. Demaria[a], L. Finco[a,b], C. Mariotti[a], S. Maselli[a], E. Migliore[a,b], V. Monaco[a,b], M. Musich[a], M.M. Obertino[a,c], G. Ortona[a,b], L. Pacher[a,b], N. Pastrone[a], M. Pelliccioni[a,2], G.L. Pinna Angioni[a,b], A. Potenza[a,b], A. Romero[a,b], M. Ruspa[a,c], R. Sacchi[a,b], A. Solano[a,b], A. Staiano[a], U. Tamponi[a]

INFN Sezione di Trieste [a]**, Università di Trieste** [b]**, Trieste, Italy**
S. Belforte[a], V. Candelise[a,b], M. Casarsa[a], F. Cossutti[a], G. Della Ricca[a,b], B. Gobbo[a], C. La Licata[a,b], M. Marone[a,b], D. Montanino[a,b], A. Schizzi[a,b], T. Umer[a,b], A. Zanetti[a]

Kangwon National University, Chunchon, Korea
S. Chang, S.K. Nam

Kyungpook National University, Daegu, Korea
D.H. Kim, G.N. Kim, M.S. Kim, D.J. Kong, S. Lee, Y.D. Oh, H. Park, A. Sakharov, D.C. Son

Chonnam National University, Institute for Universe and Elementary Particles, Kwangju, Korea
J.Y. Kim, S. Song

Korea University, Seoul, Korea
S. Choi, D. Gyun, B. Hong, M. Jo, H. Kim, Y. Kim, B. Lee, K.S. Lee, S.K. Park, Y. Roh

University of Seoul, Seoul, Korea
M. Choi, J.H. Kim, I.C. Park, S. Park, G. Ryu, M.S. Ryu

Sungkyunkwan University, Suwon, Korea
Y. Choi, Y.K. Choi, J. Goh, E. Kwon, J. Lee, H. Seo, I. Yu

Vilnius University, Vilnius, Lithuania
A. Juodagalvis

National Centre for Particle Physics, Universiti Malaya, Kuala Lumpur, Malaysia
J.R. Komaragiri

Centro de Investigacion y de Estudios Avanzados del IPN, Mexico City, Mexico
H. Castilla-Valdez, E. De La Cruz-Burelo, I. Heredia-de La Cruz[31], R. Lopez-Fernandez, J. Martínez-Ortega, A. Sanchez-Hernandez, L.M. Villasenor-Cendejas

Universidad Iberoamericana, Mexico City, Mexico
S. Carrillo Moreno, F. Vazquez Valencia

Benemerita Universidad Autonoma de Puebla, Puebla, Mexico
I. Pedraza, H.A. Salazar Ibarguen

Universidad Autónoma de San Luis Potosí, San Luis Potosí, Mexico
E. Casimiro Linares, A. Morelos Pineda

University of Auckland, Auckland, New Zealand
D. Krofcheck

University of Canterbury, Christchurch, New Zealand
P.H. Butler, S. Reucroft

National Centre for Physics, Quaid-I-Azam University, Islamabad, Pakistan
A. Ahmad, M. Ahmad, Q. Hassan, H.R. Hoorani, S. Khalid, W.A. Khan, T. Khurshid, M.A. Shah, M. Shoaib

National Centre for Nuclear Research, Swierk, Poland
H. Bialkowska, M. Bluj[32], B. Boimska, T. Frueboes, M. Górski, M. Kazana, K. Nawrocki, K. Romanowska-Rybinska, M. Szleper, P. Zalewski

Institute of Experimental Physics, Faculty of Physics, University of Warsaw, Warsaw, Poland
G. Brona, K. Bunkowski, M. Cwiok, W. Dominik, K. Doroba, A. Kalinowski, M. Konecki, J. Krolikowski, M. Misiura, M. Olszewski, W. Wolszczak

Laboratório de Instrumentação e Física Experimental de Partículas, Lisboa, Portugal
P. Bargassa, C. Beirão Da Cruz E Silva, P. Faccioli, P.G. Ferreira Parracho, M. Gallinaro, F. Nguyen, J. Rodrigues Antunes, J. Seixas, J. Varela, P. Vischia

Joint Institute for Nuclear Research, Dubna, Russia
S. Afanasiev, P. Bunin, M. Gavrilenko, I. Golutvin, I. Gorbunov, A. Kamenev, V. Karjavin, V. Konoplyanikov, A. Lanev, A. Malakhov, V. Matveev[33], P. Moisenz, V. Palichik, V. Perelygin, S. Shmatov, N. Skatchkov, V. Smirnov, A. Zarubin

Petersburg Nuclear Physics Institute, Gatchina (St. Petersburg), Russia
V. Golovtsov, Y. Ivanov, V. Kim[34], P. Levchenko, V. Murzin, V. Oreshkin, I. Smirnov, V. Sulimov, L. Uvarov, S. Vavilov, A. Vorobyev, An. Vorobyev

Institute for Nuclear Research, Moscow, Russia
Yu. Andreev, A. Dermenev, S. Gninenko, N. Golubev, M. Kirsanov, N. Krasnikov, A. Pashenkov, D. Tlisov, A. Toropin

Institute for Theoretical and Experimental Physics, Moscow, Russia
V. Epshteyn, V. Gavrilov, N. Lychkovskaya, V. Popov, G. Safronov, S. Semenov, A. Spiridonov, V. Stolin, E. Vlasov, A. Zhokin

P.N. Lebedev Physical Institute, Moscow, Russia
V. Andreev, M. Azarkin, I. Dremin, M. Kirakosyan, A. Leonidov, G. Mesyats, S.V. Rusakov, A. Vinogradov

Skobeltsyn Institute of Nuclear Physics, Lomonosov Moscow State University, Moscow, Russia
A. Belyaev, E. Boos, M. Dubinin[7], L. Dudko, A. Ershov, A. Gribushin, V. Klyukhin, O. Kodolova, I. Lokhtin, S. Obraztsov, S. Petrushanko, V. Savrin, A. Snigirev

State Research Center of Russian Federation, Institute for High Energy Physics, Protvino, Russia
I. Azhgirey, I. Bayshev, S. Bitioukov, V. Kachanov, A. Kalinin, D. Konstantinov, V. Krychkine, V. Petrov, R. Ryutin, A. Sobol, L. Tourtchanovitch, S. Troshin, N. Tyurin, A. Uzunian, A. Volkov

University of Belgrade, Faculty of Physics and Vinca Institute of Nuclear Sciences, Belgrade, Serbia
P. Adzic[35], M. Djordjevic, M. Ekmedzic, J. Milosevic

Centro de Investigaciones Energéticas Medioambientales y Tecnológicas (CIEMAT), Madrid, Spain
J. Alcaraz Maestre, C. Battilana, E. Calvo, M. Cerrada, M. Chamizo Llatas[2], N. Colino, B. De La Cruz, A. Delgado Peris, D. Domínguez Vázquez, A. Escalante Del Valle, C. Fernandez Bedoya, J.P. Fernández Ramos, J. Flix, M.C. Fouz, P. Garcia-Abia, O. Gonzalez Lopez, S. Goy Lopez, J.M. Hernandez, M.I. Josa, G. Merino, E. Navarro De Martino, A. Pérez-Calero Yzquierdo, J. Puerta Pelayo, A. Quintario Olmeda, I. Redondo, L. Romero, M.S. Soares

Universidad Autónoma de Madrid, Madrid, Spain
C. Albajar, J.F. de Trocóniz, M. Missiroli

Universidad de Oviedo, Oviedo, Spain
H. Brun, J. Cuevas, J. Fernandez Menendez, S. Folgueras, I. Gonzalez Caballero, L. Lloret Iglesias

Instituto de Física de Cantabria (IFCA), CSIC-Universidad de Cantabria, Santander, Spain
J.A. Brochero Cifuentes, I.J. Cabrillo, A. Calderon, J. Duarte Campderros, M. Fernandez, G. Gomez, J. Gonzalez Sanchez, A. Graziano, A. Lopez Virto, J. Marco, R. Marco, C. Martinez Rivero, F. Matorras, F.J. Munoz Sanchez, J. Piedra Gomez, T. Rodrigo, A.Y. Rodríguez-Marrero, A. Ruiz-Jimeno, L. Scodellaro, I. Vila, R. Vilar Cortabitarte

CERN, European Organization for Nuclear Research, Geneva, Switzerland
D. Abbaneo, E. Auffray, G. Auzinger, M. Bachtis, P. Baillon, A.H. Ball, D. Barney, A. Benaglia, J. Bendavid, L. Benhabib, J.F. Benitez, C. Bernet[8], G. Bianchi, P. Bloch, A. Bocci, A. Bonato, O. Bondu, C. Botta, H. Breuker, T. Camporesi, G. Cerminara, T. Christiansen, S. Colafranceschi[36], M. D'Alfonso, D. d'Enterria, A. Dabrowski, A. David, F. De Guio, A. De Roeck, S. De Visscher, M. Dobson, N. Dupont-Sagorin, A. Elliott-Peisert, J. Eugster, G. Franzoni, W. Funk, M. Giffels, D. Gigi, K. Gill, D. Giordano, M. Girone, F. Glege, R. Guida, J. Hammer, M. Hansen, P. Harris, J. Hegeman, V. Innocente, P. Janot, E. Karavakis, K. Kousouris, K. Krajczar, P. Lecoq, C. Lourenço, N. Magini, L. Malgeri, M. Mannelli, L. Masetti, F. Meijers, S. Mersi, E. Meschi, F. Moortgat, M. Mulders, P. Musella, L. Orsini, L. Pape, E. Perez, L. Perrozzi, A. Petrilli, G. Petrucciani, A. Pfeiffer, M. Pierini, M. Pimiä, D. Piparo, M. Plagge, A. Racz, G. Rolandi[37], M. Rovere, H. Sakulin, C. Schäfer, C. Schwick, S. Sekmen, A. Sharma, P. Siegrist, P. Silva, M. Simon, P. Sphicas[38], D. Spiga, J. Steggemann, B. Stieger, M. Stoye, D. Treille, A. Tsirou, G.I. Veres[19], J.R. Vlimant, H.K. Wöhri, W.D. Zeuner

Paul Scherrer Institut, Villigen, Switzerland
W. Bertl, K. Deiters, W. Erdmann, R. Horisberger, Q. Ingram, H.C. Kaestli, S. König, D. Kotlinski, U. Langenegger, D. Renker, T. Rohe

Institute for Particle Physics, ETH Zurich, Zurich, Switzerland

F. Bachmair, L. Bäni, L. Bianchini, P. Bortignon, M.A. Buchmann, B. Casal, N. Chanon, A. Deisher, G. Dissertori, M. Dittmar, M. Donegà, M. Dünser, P. Eller, C. Grab, D. Hits, W. Lustermann, B. Mangano, A.C. Marini, P. Martinez Ruiz del Arbol, D. Meister, N. Mohr, C. Nägeli[39], P. Nef, F. Nessi-Tedaldi, F. Pandolfi, F. Pauss, M. Peruzzi, M. Quittnat, L. Rebane, F.J. Ronga, M. Rossini, A. Starodumov[40], M. Takahashi, K. Theofilatos, R. Wallny, H.A. Weber

Universität Zürich, Zurich, Switzerland

C. Amsler[41], M.F. Canelli, V. Chiochia, A. De Cosa, A. Hinzmann, T. Hreus, M. Ivova Rikova, B. Kilminster, B. Millan Mejias, J. Ngadiuba, P. Robmann, H. Snoek, S. Taroni, M. Verzetti, Y. Yang

National Central University, Chung-Li, Taiwan

M. Cardaci, K.H. Chen, C. Ferro, C.M. Kuo, W. Lin, Y.J. Lu, R. Volpe, S.S. Yu

National Taiwan University (NTU), Taipei, Taiwan

P. Chang, Y.H. Chang, Y.W. Chang, Y. Chao, K.F. Chen, P.H. Chen, C. Dietz, U. Grundler, W.-S. Hou, K.Y. Kao, Y.J. Lei, Y.F. Liu, R.-S. Lu, D. Majumder, E. Petrakou, X. Shi, Y.M. Tzeng, R. Wilken

Chulalongkorn University, Bangkok, Thailand

B. Asavapibhop, N. Srimanobhas, N. Suwonjandee

Cukurova University, Adana, Turkey

A. Adiguzel, M.N. Bakirci[42], S. Cerci[43], C. Dozen, I. Dumanoglu, E. Eskut, S. Girgis, G. Gokbulut, E. Gurpinar, I. Hos, E.E. Kangal, A. Kayis Topaksu, G. Onengut[44], K. Ozdemir, S. Ozturk[42], A. Polatoz, K. Sogut[45], D. Sunar Cerci[43], B. Tali[43], H. Topakli[42], M. Vergili

Middle East Technical University, Physics Department, Ankara, Turkey

I.V. Akin, B. Bilin, S. Bilmis, H. Gamsizkan, G. Karapinar[46], K. Ocalan, U.E. Surat, M. Yalvac, M. Zeyrek

Bogazici University, Istanbul, Turkey

E. Gülmez, B. Isildak[47], M. Kaya[48], O. Kaya[48]

Istanbul Technical University, Istanbul, Turkey

H. Bahtiyar[49], E. Barlas, K. Cankocak, F.I. Vardarlı, M. Yücel

National Scientific Center, Kharkov Institute of Physics and Technology, Kharkov, Ukraine

L. Levchuk, P. Sorokin

University of Bristol, Bristol, United Kingdom

J.J. Brooke, E. Clement, D. Cussans, H. Flacher, R. Frazier, J. Goldstein, M. Grimes, G.P. Heath, H.F. Heath, J. Jacob, L. Kreczko, C. Lucas, Z. Meng, D.M. Newbold[50], S. Paramesvaran, A. Poll, S. Senkin, V.J. Smith, T. Williams

Rutherford Appleton Laboratory, Didcot, United Kingdom

K.W. Bell, A. Belyaev[51], C. Brew, R.M. Brown, D.J.A. Cockerill, J.A. Coughlan, K. Harder, S. Harper, E. Olaiya, D. Petyt, C.H. Shepherd-Themistocleous, A. Thea, I.R. Tomalin, W.J. Womersley, S.D. Worm

Imperial College, London, United Kingdom

M. Baber, R. Bainbridge, O. Buchmuller, D. Burton, D. Colling, N. Cripps, M. Cutajar, P. Dauncey, G. Davies, M. Della Negra, P. Dunne, W. Ferguson, J. Fulcher, D. Futyan, A. Gilbert, A. Guneratne Bryer, G. Hall, Z. Hatherell, G. Iles, M. Jarvis, G. Karapostoli, M. Kenzie, R. Lane,

R. Lucas[50], L. Lyons, A.-M. Magnan, S. Malik, J. Marrouche, B. Mathias, R. Nandi, J. Nash, A. Nikitenko[40], J. Pela, M. Pesaresi, K. Petridis, D.M. Raymond, S. Rogerson, A. Rose, C. Seez, P. Sharp[†], A. Sparrow, A. Tapper, M. Vazquez Acosta, T. Virdee, S. Wakefield

Brunel University, Uxbridge, United Kingdom
J.E. Cole, P.R. Hobson, A. Khan, P. Kyberd, D. Leggat, D. Leslie, W. Martin, I.D. Reid, P. Symonds, L. Teodorescu, M. Turner

Baylor University, Waco, USA
J. Dittmann, K. Hatakeyama, A. Kasmi, H. Liu, T. Scarborough

The University of Alabama, Tuscaloosa, USA
O. Charaf, S.I. Cooper, C. Henderson, P. Rumerio

Boston University, Boston, USA
A. Avetisyan, T. Bose, C. Fantasia, A. Heister, P. Lawson, C. Richardson, J. Rohlf, D. Sperka, J. St. John, L. Sulak

Brown University, Providence, USA
J. Alimena, S. Bhattacharya, G. Christopher, D. Cutts, Z. Demiragli, A. Ferapontov, A. Garabedian, U. Heintz, S. Jabeen, G. Kukartsev, E. Laird, G. Landsberg, M. Luk, M. Narain, M. Segala, T. Sinthuprasith, T. Speer, J. Swanson

University of California, Davis, Davis, USA
R. Breedon, G. Breto, M. Calderon De La Barca Sanchez, S. Chauhan, M. Chertok, J. Conway, R. Conway, P.T. Cox, R. Erbacher, M. Gardner, W. Ko, A. Kopecky, R. Lander, T. Miceli, M. Mulhearn, D. Pellett, J. Pilot, F. Ricci-Tam, B. Rutherford, M. Searle, S. Shalhout, J. Smith, M. Squires, M. Tripathi, S. Wilbur, R. Yohay

University of California, Los Angeles, USA
R. Cousins, P. Everaerts, C. Farrell, J. Hauser, M. Ignatenko, G. Rakness, E. Takasugi, V. Valuev, M. Weber

University of California, Riverside, Riverside, USA
J. Babb, R. Clare, J. Ellison, J.W. Gary, G. Hanson, J. Heilman, P. Jandir, F. Lacroix, H. Liu, O.R. Long, A. Luthra, M. Malberti, H. Nguyen, A. Shrinivas, J. Sturdy, S. Sumowidagdo, S. Wimpenny

University of California, San Diego, La Jolla, USA
W. Andrews, J.G. Branson, G.B. Cerati, S. Cittolin, R.T. D'Agnolo, D. Evans, A. Holzner, R. Kelley, M. Lebourgeois, J. Letts, I. Macneill, S. Padhi, C. Palmer, M. Pieri, M. Sani, V. Sharma, S. Simon, E. Sudano, M. Tadel, Y. Tu, A. Vartak, F. Würthwein, A. Yagil, J. Yoo

University of California, Santa Barbara, Santa Barbara, USA
D. Barge, J. Bradmiller-Feld, C. Campagnari, T. Danielson, A. Dishaw, K. Flowers, M. Franco Sevilla, P. Geffert, C. George, F. Golf, J. Incandela, C. Justus, N. Mccoll, J. Richman, D. Stuart, W. To, C. West

California Institute of Technology, Pasadena, USA
A. Apresyan, A. Bornheim, J. Bunn, Y. Chen, E. Di Marco, J. Duarte, A. Mott, H.B. Newman, C. Pena, C. Rogan, M. Spiropulu, V. Timciuc, R. Wilkinson, S. Xie, R.Y. Zhu

Carnegie Mellon University, Pittsburgh, USA
V. Azzolini, A. Calamba, R. Carroll, T. Ferguson, Y. Iiyama, M. Paulini, J. Russ, H. Vogel, I. Vorobiev

University of Colorado at Boulder, Boulder, USA
J.P. Cumalat, B.R. Drell, W.T. Ford, A. Gaz, E. Luiggi Lopez, U. Nauenberg, J.G. Smith, K. Stenson, K.A. Ulmer, S.R. Wagner

Cornell University, Ithaca, USA
J. Alexander, A. Chatterjee, J. Chu, N. Eggert, W. Hopkins, A. Khukhunaishvili, B. Kreis, N. Mirman, G. Nicolas Kaufman, J.R. Patterson, A. Ryd, E. Salvati, L. Skinnari, W. Sun, W.D. Teo, J. Thom, J. Thompson, J. Tucker, Y. Weng, L. Winstrom, P. Wittich

Fairfield University, Fairfield, USA
D. Winn

Fermi National Accelerator Laboratory, Batavia, USA
S. Abdullin, M. Albrow, J. Anderson, G. Apollinari, L.A.T. Bauerdick, A. Beretvas, J. Berryhill, P.C. Bhat, K. Burkett, J.N. Butler, H.W.K. Cheung, F. Chlebana, S. Cihangir, V.D. Elvira, I. Fisk, J. Freeman, E. Gottschalk, L. Gray, D. Green, S. Grünendahl, O. Gutsche, J. Hanlon, D. Hare, R.M. Harris, J. Hirschauer, B. Hooberman, S. Jindariani, M. Johnson, U. Joshi, K. Kaadze, B. Klima, S. Kwan, J. Linacre, D. Lincoln, R. Lipton, T. Liu, J. Lykken, K. Maeshima, J.M. Marraffino, V.I. Martinez Outschoorn, S. Maruyama, D. Mason, P. McBride, K. Mishra, S. Mrenna, Y. Musienko[33], S. Nahn, C. Newman-Holmes, V. O'Dell, O. Prokofyev, E. Sexton-Kennedy, S. Sharma, A. Soha, W.J. Spalding, L. Spiegel, L. Taylor, S. Tkaczyk, N.V. Tran, L. Uplegger, E.W. Vaandering, R. Vidal, J. Whitmore, F. Yang

University of Florida, Gainesville, USA
D. Acosta, P. Avery, D. Bourilkov, T. Cheng, S. Das, M. De Gruttola, G.P. Di Giovanni, D. Dobur, R.D. Field, M. Fisher, I.K. Furic, J. Hugon, J. Konigsberg, A. Korytov, A. Kropivnitskaya, T. Kypreos, J.F. Low, K. Matchev, P. Milenovic[52], G. Mitselmakher, L. Muniz, A. Rinkevicius, L. Shchutska, N. Skhirtladze, M. Snowball, J. Yelton, M. Zakaria

Florida International University, Miami, USA
V. Gaultney, S. Hewamanage, S. Linn, P. Markowitz, G. Martinez, J.L. Rodriguez

Florida State University, Tallahassee, USA
T. Adams, A. Askew, J. Bochenek, B. Diamond, J. Haas, S. Hagopian, V. Hagopian, K.F. Johnson, H. Prosper, V. Veeraraghavan, M. Weinberg

Florida Institute of Technology, Melbourne, USA
M.M. Baarmand, M. Hohlmann, H. Kalakhety, F. Yumiceva

University of Illinois at Chicago (UIC), Chicago, USA
M.R. Adams, L. Apanasevich, V.E. Bazterra, R.R. Betts, I. Bucinskaite, R. Cavanaugh, O. Evdokimov, L. Gauthier, C.E. Gerber, D.J. Hofman, S. Khalatyan, P. Kurt, D.H. Moon, C. O'Brien, C. Silkworth, P. Turner, N. Varelas

The University of Iowa, Iowa City, USA
E.A. Albayrak[49], B. Bilki[53], W. Clarida, K. Dilsiz, F. Duru, M. Haytmyradov, J.-P. Merlo, H. Mermerkaya[54], A. Mestvirishvili, A. Moeller, J. Nachtman, H. Ogul, Y. Onel, F. Ozok[49], A. Penzo, R. Rahmat, S. Sen, P. Tan, E. Tiras, J. Wetzel, T. Yetkin[55], K. Yi

Johns Hopkins University, Baltimore, USA
B.A. Barnett, B. Blumenfeld, D. Fehling, A.V. Gritsan, P. Maksimovic, C. Martin, M. Swartz

The University of Kansas, Lawrence, USA
P. Baringer, A. Bean, G. Benelli, J. Gray, R.P. Kenny III, M. Murray, D. Noonan, S. Sanders, J. Sekaric, R. Stringer, Q. Wang, J.S. Wood

Kansas State University, Manhattan, USA
A.F. Barfuss, I. Chakaberia, A. Ivanov, S. Khalil, M. Makouski, Y. Maravin, L.K. Saini, S. Shrestha, I. Svintradze

Lawrence Livermore National Laboratory, Livermore, USA
J. Gronberg, D. Lange, F. Rebassoo, D. Wright

University of Maryland, College Park, USA
A. Baden, B. Calvert, S.C. Eno, J.A. Gomez, N.J. Hadley, R.G. Kellogg, T. Kolberg, Y. Lu, M. Marionneau, A.C. Mignerey, K. Pedro, A. Skuja, M.B. Tonjes, S.C. Tonwar

Massachusetts Institute of Technology, Cambridge, USA
A. Apyan, R. Barbieri, G. Bauer, W. Busza, I.A. Cali, M. Chan, L. Di Matteo, V. Dutta, G. Gomez Ceballos, M. Goncharov, D. Gulhan, M. Klute, Y.S. Lai, Y.-J. Lee, A. Levin, P.D. Luckey, T. Ma, C. Paus, D. Ralph, C. Roland, G. Roland, G.S.F. Stephans, F. Stöckli, K. Sumorok, D. Velicanu, J. Veverka, B. Wyslouch, M. Yang, M. Zanetti, V. Zhukova

University of Minnesota, Minneapolis, USA
B. Dahmes, A. De Benedetti, A. Gude, S.C. Kao, K. Klapoetke, Y. Kubota, J. Mans, N. Pastika, R. Rusack, A. Singovsky, N. Tambe, J. Turkewitz

University of Mississippi, Oxford, USA
J.G. Acosta, S. Oliveros

University of Nebraska-Lincoln, Lincoln, USA
E. Avdeeva, K. Bloom, S. Bose, D.R. Claes, A. Dominguez, R. Gonzalez Suarez, J. Keller, D. Knowlton, I. Kravchenko, J. Lazo-Flores, S. Malik, F. Meier, G.R. Snow

State University of New York at Buffalo, Buffalo, USA
J. Dolen, A. Godshalk, I. Iashvili, A. Kharchilava, A. Kumar, S. Rappoccio

Northeastern University, Boston, USA
G. Alverson, E. Barberis, D. Baumgartel, M. Chasco, J. Haley, A. Massironi, D.M. Morse, D. Nash, T. Orimoto, D. Trocino, D. Wood, J. Zhang

Northwestern University, Evanston, USA
K.A. Hahn, A. Kubik, N. Mucia, N. Odell, B. Pollack, A. Pozdnyakov, M. Schmitt, S. Stoynev, K. Sung, M. Velasco, S. Won

University of Notre Dame, Notre Dame, USA
D. Berry, A. Brinkerhoff, K.M. Chan, A. Drozdetskiy, M. Hildreth, C. Jessop, D.J. Karmgard, N. Kellams, K. Lannon, W. Luo, S. Lynch, N. Marinelli, T. Pearson, M. Planer, R. Ruchti, N. Valls, M. Wayne, M. Wolf, A. Woodard

The Ohio State University, Columbus, USA
L. Antonelli, B. Bylsma, L.S. Durkin, S. Flowers, C. Hill, R. Hughes, K. Kotov, T.Y. Ling, D. Puigh, M. Rodenburg, G. Smith, C. Vuosalo, B.L. Winer, H. Wolfe, H.W. Wulsin

Princeton University, Princeton, USA
E. Berry, P. Elmer, P. Hebda, A. Hunt, S.A. Koay, P. Lujan, D. Marlow, T. Medvedeva, M. Mooney, J. Olsen, P. Piroué, X. Quan, H. Saka, D. Stickland, C. Tully, J.S. Werner, S.C. Zenz, A. Zuranski

University of Puerto Rico, Mayaguez, USA
E. Brownson, H. Mendez, J.E. Ramirez Vargas

Purdue University, West Lafayette, USA
E. Alagoz, V.E. Barnes, D. Benedetti, G. Bolla, D. Bortoletto, M. De Mattia, A. Everett, Z. Hu, M.K. Jha, M. Jones, K. Jung, M. Kress, N. Leonardo, D. Lopes Pegna, V. Maroussov, P. Merkel, D.H. Miller, N. Neumeister, B.C. Radburn-Smith, I. Shipsey, D. Silvers, A. Svyatkovskiy, F. Wang, W. Xie, L. Xu, H.D. Yoo, J. Zablocki, Y. Zheng

Purdue University Calumet, Hammond, USA
N. Parashar, J. Stupak

Rice University, Houston, USA
A. Adair, B. Akgun, K.M. Ecklund, F.J.M. Geurts, W. Li, B. Michlin, B.P. Padley, R. Redjimi, J. Roberts, J. Zabel

University of Rochester, Rochester, USA
B. Betchart, A. Bodek, R. Covarelli, P. de Barbaro, R. Demina, Y. Eshaq, T. Ferbel, A. Garcia-Bellido, P. Goldenzweig, J. Han, A. Harel, D.C. Miner, G. Petrillo, D. Vishnevskiy

The Rockefeller University, New York, USA
R. Ciesielski, L. Demortier, K. Goulianos, G. Lungu, C. Mesropian

Rutgers, The State University of New Jersey, Piscataway, USA
S. Arora, A. Barker, J.P. Chou, C. Contreras-Campana, E. Contreras-Campana, D. Duggan, D. Ferencek, Y. Gershtein, R. Gray, E. Halkiadakis, D. Hidas, A. Lath, S. Panwalkar, M. Park, R. Patel, V. Rekovic, S. Salur, S. Schnetzer, C. Seitz, S. Somalwar, R. Stone, S. Thomas, P. Thomassen, M. Walker

University of Tennessee, Knoxville, USA
K. Rose, S. Spanier, A. York

Texas A&M University, College Station, USA
O. Bouhali[56], R. Eusebi, W. Flanagan, J. Gilmore, T. Kamon[57], V. Khotilovich, V. Krutelyov, R. Montalvo, I. Osipenkov, Y. Pakhotin, A. Perloff, J. Roe, A. Rose, A. Safonov, T. Sakuma, I. Suarez, A. Tatarinov

Texas Tech University, Lubbock, USA
N. Akchurin, C. Cowden, J. Damgov, C. Dragoiu, P.R. Dudero, J. Faulkner, K. Kovitanggoon, S. Kunori, S.W. Lee, T. Libeiro, I. Volobouev

Vanderbilt University, Nashville, USA
E. Appelt, A.G. Delannoy, S. Greene, A. Gurrola, W. Johns, C. Maguire, Y. Mao, A. Melo, M. Sharma, P. Sheldon, B. Snook, S. Tuo, J. Velkovska

University of Virginia, Charlottesville, USA
M.W. Arenton, S. Boutle, B. Cox, B. Francis, J. Goodell, R. Hirosky, A. Ledovskoy, H. Li, C. Lin, C. Neu, J. Wood

Wayne State University, Detroit, USA
S. Gollapinni, R. Harr, P.E. Karchin, C. Kottachchi Kankanamge Don, P. Lamichhane

University of Wisconsin, Madison, USA
D.A. Belknap, D. Carlsmith, M. Cepeda, S. Dasu, S. Duric, E. Friis, R. Hall-Wilton, M. Herndon, A. Hervé, P. Klabbers, J. Klukas, A. Lanaro, C. Lazaridis, A. Levine, R. Loveless, A. Mohapatra, I. Ojalvo, T. Perry, G.A. Pierro, G. Polese, I. Ross, T. Sarangi, A. Savin, W.H. Smith, N. Woods

†: Deceased
1: Also at Vienna University of Technology, Vienna, Austria

2: Also at CERN, European Organization for Nuclear Research, Geneva, Switzerland
3: Also at Institut Pluridisciplinaire Hubert Curien, Université de Strasbourg, Université de Haute Alsace Mulhouse, CNRS/IN2P3, Strasbourg, France
4: Also at National Institute of Chemical Physics and Biophysics, Tallinn, Estonia
5: Also at Skobeltsyn Institute of Nuclear Physics, Lomonosov Moscow State University, Moscow, Russia
6: Also at Universidade Estadual de Campinas, Campinas, Brazil
7: Also at California Institute of Technology, Pasadena, USA
8: Also at Laboratoire Leprince-Ringuet, Ecole Polytechnique, IN2P3-CNRS, Palaiseau, France
9: Also at Suez University, Suez, Egypt
10: Also at Cairo University, Cairo, Egypt
11: Also at Fayoum University, El-Fayoum, Egypt
12: Also at British University in Egypt, Cairo, Egypt
13: Now at Ain Shams University, Cairo, Egypt
14: Also at Université de Haute Alsace, Mulhouse, France
15: Also at Joint Institute for Nuclear Research, Dubna, Russia
16: Also at Brandenburg University of Technology, Cottbus, Germany
17: Also at The University of Kansas, Lawrence, USA
18: Also at Institute of Nuclear Research ATOMKI, Debrecen, Hungary
19: Also at Eötvös Loránd University, Budapest, Hungary
20: Also at University of Debrecen, Debrecen, Hungary
21: Also at Tata Institute of Fundamental Research - HECR, Mumbai, India
22: Now at King Abdulaziz University, Jeddah, Saudi Arabia
23: Also at University of Visva-Bharati, Santiniketan, India
24: Also at University of Ruhuna, Matara, Sri Lanka
25: Also at Isfahan University of Technology, Isfahan, Iran
26: Also at Sharif University of Technology, Tehran, Iran
27: Also at Plasma Physics Research Center, Science and Research Branch, Islamic Azad University, Tehran, Iran
28: Also at Università degli Studi di Siena, Siena, Italy
29: Also at Centre National de la Recherche Scientifique (CNRS) - IN2P3, Paris, France
30: Also at Purdue University, West Lafayette, USA
31: Also at Universidad Michoacana de San Nicolas de Hidalgo, Morelia, Mexico
32: Also at National Centre for Nuclear Research, Swierk, Poland
33: Also at Institute for Nuclear Research, Moscow, Russia
34: Also at St. Petersburg State Polytechnical University, St. Petersburg, Russia
35: Also at Faculty of Physics, University of Belgrade, Belgrade, Serbia
36: Also at Facoltà Ingegneria, Università di Roma, Roma, Italy
37: Also at Scuola Normale e Sezione dell'INFN, Pisa, Italy
38: Also at University of Athens, Athens, Greece
39: Also at Paul Scherrer Institut, Villigen, Switzerland
40: Also at Institute for Theoretical and Experimental Physics, Moscow, Russia
41: Also at Albert Einstein Center for Fundamental Physics, Bern, Switzerland
42: Also at Gaziosmanpasa University, Tokat, Turkey
43: Also at Adiyaman University, Adiyaman, Turkey
44: Also at Cag University, Mersin, Turkey
45: Also at Mersin University, Mersin, Turkey
46: Also at Izmir Institute of Technology, Izmir, Turkey
47: Also at Ozyegin University, Istanbul, Turkey

48: Also at Kafkas University, Kars, Turkey

49: Also at Mimar Sinan University, Istanbul, Istanbul, Turkey

50: Also at Rutherford Appleton Laboratory, Didcot, United Kingdom

51: Also at School of Physics and Astronomy, University of Southampton, Southampton, United Kingdom

52: Also at University of Belgrade, Faculty of Physics and Vinca Institute of Nuclear Sciences, Belgrade, Serbia

53: Also at Argonne National Laboratory, Argonne, USA

54: Also at Erzincan University, Erzincan, Turkey

55: Also at Yildiz Technical University, Istanbul, Turkey

56: Also at Texas A&M University at Qatar, Doha, Qatar

57: Also at Kyungpook National University, Daegu, Korea